ISSN 2220-315x (online)

World Journal of *Experimental Medicine*

World J Exp Med 2022 July 20; 12(4): 53-91

Published by Baishideng Publishing Group Inc

World Journal of Experimental Medicine

Contents

Bimonthly Volume 12 Number 4 July 20, 2022

REVIEW

ORIGINAL ARTICLE

Randomized Controlled Trial

World Journal of Experimental Medicine

Bimonthly Volume 12 Number 4 July 20, 2022

Contents

ABOUT COVER

AIMS AND SCOPE

The primary aim of the *World Journal of Experimental Medicine* (*WJEM*, *World J Exp Med*) is to provide scholars and readers from various fields of experimental medicine with a platform to publish high-quality basic and clinical research articles and communicate their research findings online.

WJEM mainly publishes articles reporting research results and findings obtained in the field of experimental medicine and covering a wide range of topics including clinical laboratory medicine (applied and basic research in hematology, body fluid examination, cytomorphology, genetic diagnosis of hematological disorders, thrombosis and hemostasis, and blood typing and transfusion), biochemical examination (applied and basic research in laboratory automation and information system, biochemical methodology, and biochemical diagnostics), *etc*.

INDEXING/ABSTRACTING

The *WJEM* is now abstracted and indexed in PubMed, PubMed Central, Scopus, Reference Citation Analysis, China National Knowledge Infrastructure, China Science and Technology Journal Database, and Superstar Journals Database.

RESPONSIBLE EDITORS FOR THIS ISSUE

NAME OF JOURNAL
World Journal of Experimental Medicine

ISSN
ISSN 2220-315x (online)

LAUNCH DATE
December 20, 2011

FREQUENCY
Bimonthly

EDITORS-IN-CHIEF
Leonardo Roever

EDITORIAL BOARD MEMBERS
https://www.wjgnet.com/2220-315x/editorialboard.htm

PUBLICATION DATE
July 20, 2022

INSTRUCTIONS TO AUTHORS
https://www.wjgnet.com/bpg/gerinfo/204

GUIDELINES FOR ETHICS DOCUMENTS
https://www.wjgnet.com/bpg/GerInfo/287

GUIDELINES FOR NON-NATIVE SPEAKERS OF ENGLISH
https://www.wjgnet.com/bpg/gerinfo/240

PUBLICATION ETHICS
https://www.wjgnet.com/bpg/GerInfo/288

PUBLICATION MISCONDUCT
https://www.wjgnet.com/bpg/gerinfo/208

ARTICLE PROCESSING CHARGE
https://www.wjgnet.com/bpg/gerinfo/242

STEPS FOR SUBMITTING MANUSCRIPTS
https://www.wjgnet.com/bpg/GerInfo/239

ONLINE SUBMISSION
https://www.f6publishing.com

World Journal of Experimental Medicine

Submit a Manuscript: https://www.f6publishing.com

World J Exp Med 2022 July 20; 12(4): 53-67

DOI: 10.5493/wjem.v12.i4.53

ISSN 2220-315x (online)

REVIEW

Complement-mediated microvascular injury and thrombosis in the pathogenesis of severe COVID-19: A review

Panagiota Gianni, Mark Goldin, Sam Ngu, Stefanos Zafeiropoulos, Georgios Geropoulos, Dimitrios Giannis

Specialty type: Immunology

Provenance and peer review: Invited article; Externally peer reviewed.

Peer-review model: Single blind

Peer-review report's scientific quality classification
Grade A (Excellent): 0
Grade B (Very good): B
Grade C (Good): C
Grade D (Fair): D
Grade E (Poor): 0

P-Reviewer: Han J, China; Papadopoulos K, Thailand
A-Editor: Zhu JQ, China

Received: February 9, 2022
Peer-review started: February 9, 2022
First decision: April 13, 2022
Revised: April 27, 2022
Accepted: June 13, 2022
Article in press: June 13, 2022
Published online: July 20, 2022

Panagiota Gianni, Department of Internal Medicine III, Hematology, Oncology, Palliative Medicine, Rheumatology and Infectious Diseases, University Hospital Ulm, Ulm 89070, Germany

Mark Goldin, Sam Ngu, Dimitrios Giannis, Donald and Barbara Zucker School of Medicine at Hofstra/Northwell, Northwell Health, New York, NY 11549, United States

Mark Goldin, Feinstein Institutes for Medical Research at Northwell Health, Feinstein Institutes , New York, NY 11030, United States

Stefanos Zafeiropoulos, Elmezzi Graduate School of Molecular Medicine, Northwell Health, New York, NY 11030, United States

Georgios Geropoulos, Department of General Surgery, University College London Hospitals, London NW12BU, United Kingdom

Dimitrios Giannis, North Shore/Long Island Jewish General Surgery, Northwell Health, New York, NY 11021, United States

Corresponding author: Dimitrios Giannis, MD, MSc, Donald and Barbara Zucker School of Medicine at Hofstra/Northwell, Northwell Health, 500 Hofstra Blvd, Hempstead, NY 11549, United States. dimitrisgiannhs@gmail.com

Abstract

Coronavirus disease 2019 (COVID-19) causes acute microvascular thrombosis in both venous and arterial structures which is highly associated with increased mortality. The mechanisms leading to thromboembolism are still under investigation. Current evidence suggests that excessive complement activation with severe amplification of the inflammatory response (cytokine storm) hastens disease progression and initiates complement-dependent cytotoxic tissue damage with resultant prothrombotic complications. The concept of thromboinflammation, involving overt inflammation and activation of the coagulation cascade causing thrombotic microangiopathy and end-organ damage, has emerged as one of the core components of COVID-19 pathogenesis. The complement system is a major mediator of the innate immune response and inflammation and thus an appealing treatment target. In this review, we discuss the role of complement in the development of thrombotic microangiopathy and summarize the current data on complement inhibitors as COVID-19 therapeutics.

Key Words: COVID-19; Complement; Microvascular injury; Thromboembolism; Cytokine storm; Thrombotic microangiopathy

Core Tip: Current evidence supports the role of excessive complement activation with subsequent illness progression and development of a complement-dependent cytotoxic tissue damage with detrimental effects in coronavirus disease 2019 (COVID-19) patients, including thromboembolic complications. Based on its role in the development of the cytokine storm and thrombogenesis in COVID-19, the complement system is an appealing treatment target with promising results from preliminary reports. Whether inhibition of upstream (C3, C1) or terminal (C5, C5a, or C5aR) components is of equal importance remains to be elucidated, however, preliminary results from several ongoing clinical trials show benefit in terms of 28-d mortality and pulmonary embolism.

Citation: Gianni P, Goldin M, Ngu S, Zafeiropoulos S, Geropoulos G, Giannis D. Complement-mediated microvascular injury and thrombosis in the pathogenesis of severe COVID-19: A review. *World J Exp Med* 2022; 12(4): 53-67
URL: https://www.wjgnet.com/2220-315x/full/v12/i4/53.htm
DOI: https://dx.doi.org/10.5493/wjem.v12.i4.53

INTRODUCTION

Coronaviruses are a large family of enveloped viruses that can cause serious respiratory infections, including severe acute respiratory syndrome (SARS), Middle East respiratory syndrome (MERS), and coronavirus disease 2019 (COVID-19) [from SARS coronavirus 2 (SARS-CoV-2)]. Although COVID-19 symptoms are often mild, up to 20%-25% of hospitalized patients require intensive care[1,2]. A substantial proportion of patients develop respiratory complications such as pneumonia and acute respiratory distress syndrome (ARDS) as part of a dysregulated systemic inflammatory response, in addition to acute renal, cardiac, and hepatic injury and disseminated intravascular coagulation[3]. Disease severity and mortality appear to be associated with patient age and comorbidities, suggesting a dynamic relationship between viral replication and host immune response. Patients with high levels of pro-inflammatory cytokines and chemokines show a greater degree of pulmonary inflammation, a phenomenon that has also been observed with SARS and MERS[4]. Although the molecular mechanisms of viral pathogenicity are not fully understood, immune-mediated damage is a major contributor to SARS-CoV-2-associated morbidity and mortality[5]. Rapid cardiorespiratory failure and multiorgan injury, common features of severe SARS-CoV-2 infection, can be partly explained by an aberrant immune response[6].

The complement system is an important part of the innate immune system and participates in the perivascular and intravascular clearance of pathogens, as well as in coagulation and fibrinolysis. In severe cases, SARS-CoV-2 induces a dysregulated immune response that becomes detrimental to the host, described as 'cytokine storm' or 'cytokine release syndrome'[7]. During cytokine storm, serum levels of complement components 3 and 4 (C3 and C4) and other components of the classical complement pathway as measured by the CH50 assay are decreased due to increased complement factor consumption[8]. Post-mortem cadaveric analysis of patients with severe SARS-CoV-2 infection has demonstrated thrombotic microangiopathy (TMA) implicating the activation of the complement cascade[9]. These observations, coupled with results of proteomic studies, highlight the role of complement activation in the pathogenesis of SARS-CoV-2[10]. In this review, we summarize the current evidence of complement involvement in microvascular injury and thrombosis in SARS-CoV-2 infection, as well as current data on complement inhibitors in the treatment of severe COVID-19.

THE ROLE OF THE COMPLEMENT SYSTEM IN VIRAL INFECTIONS

The complement system is an integral part of the innate immune system consisting of over 30 proteins. There are 3 distinct pathways of complement activation: the classical complement pathway, the alternative complement pathway, and the lectin pathway (Figure 1). The complement cascade mediates several immunoprotective and anti-inflammatory functions, enables clearance of viral pathogens and infected cells *via* opsonization, results in the formation of the C5b-9 membrane attack complex (MAC) on infected cells, targets intracellular viral components for proteasomal degradation, promotes

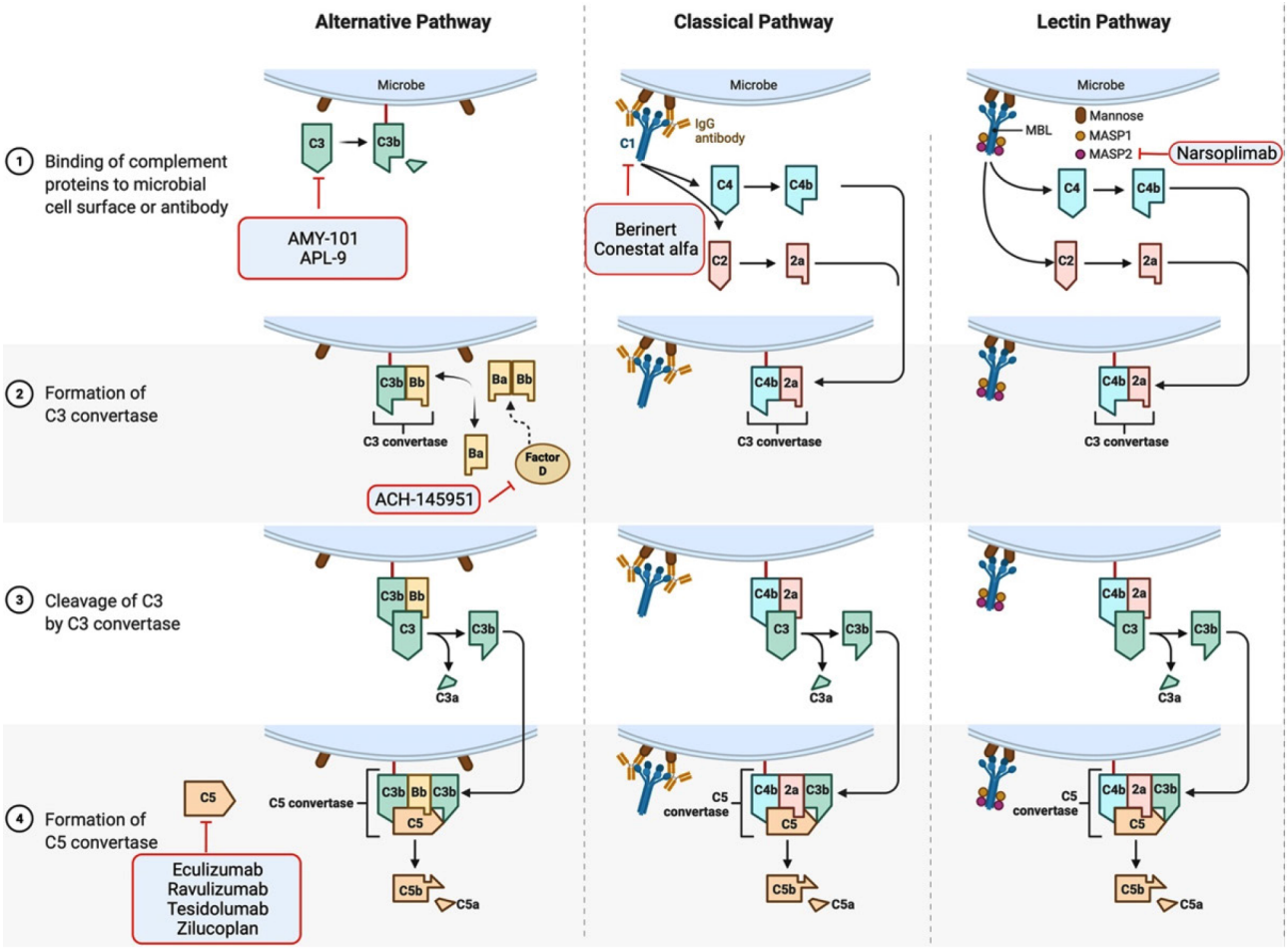

DOI: 10.5493/wjem.v12.i4.53

Figure 1 The 3 distinct pathways of complement activation (the classical complement pathway, the alternative complement pathway, and the lectin pathway) and complement inhibitors with potential use in reducing coronavirus disease 2019 related side effects. Created with BioRender.com

chemotaxis, and enhances the adaptive immune response[11]. In addition, the complement system promotes the survival of germinal center B cells and enhances the production of antigen-specific antibodies[12,13]. Further, activation of the complement system leads to the production of anaphylatoxins, such as C3a and C5a, which triggers endothelial and mast cell degranulation, enhances phagocytic activity of neutrophils and monocytes, and elicits a local inflammatory response.

Complement pathway activation plays an important role in the development of acute lung injury induced by highly pathogenic viruses, and accordingly, inhibition of complement components has been associated with protective effects[14]. High levels of C5a have been found in the upper respiratory tract and in serum samples in patients infected with the H1N1 virus and have been moderately associated with disease severity[15,16].

In preclinical studies with rodents, inhibition of C5a and upstream factors, such as C3 and C3a, reduced lung injury caused by coronavirus (SARS-CoV) and non-coronavirus (avian influenza H5N1 virus) infections[17,18]. Interestingly, there was no change in viral titers, suggesting that complement inhibition may prevent lung damage independent of viral load[17]. Further, Jiang *et al*[19] showed that MERS-CoV infection in transgenic human dipeptidyl peptidase 4 (*hDPP4*) mice was associated with elevated cytokine release and excessive complement activation, resulting in increased concentrations of C5 cleavage products in sera and lungs, while competitive antibody-mediated inhibition of the C5a receptor (C5aR) decreased viral replication and mitigated alveolar damage by limiting alveolar macrophage infiltration and interferon (IFN)-gamma receptor expression. Gralinski *et al*[17] showed significantly milder airway inflammation, decreased inflammatory cell infiltration, and lower cytokine levels in both lungs and serum of transgenic C3-deficient mice infected with SARS-CoV compared to wild-type control mice. Similar findings were observed in a primate model of influenza H7N9 virus, where inhibition of C5aR significantly decreased cytokine levels and neutrophil infiltration of the lungs [20].

COMPLEMENT ACTIVATION IN SEVERE COVID-19

Clinical studies of patients with COVID-19 have supported the theory that excessive complement activation and complement-dependent cytotoxic tissue damage drive disease progression[21]. Peffault de Latour *et al*[22] showed that the level of circulating MAC (sC5b-9) was increased in 64% of patients and plasma levels of sC5b9 were significantly higher in infected patients compared to healthy donors. Serum C5 may be associated with COVID-19 severity; those with critical disease have significantly elevated sC5b9 compared to those with mild or moderate symptoms[21,22]. Yu *et al*[23] demonstrated that serum from patients with severe COVID-19 promotes complement-mediated cell death by increasing MAC deposition on the cell surface. A positive modified Ham test (complement-mediated cell-death assay) was detected in 41.2% of intubated patients compared to 6.3% of patients requiring minimal respiratory support. Similarly, Carvelli *et al*[24] reported increased plasma C5a levels associated with disease severity and ARDS. Lastly, Holter *et al*[25] showed that sC5b9 and C4d were significantly higher in patients with respiratory failure and systemic inflammation.

The activation of the complement system results in consumption of C3 and C4 and relevant changes have been investigated as markers of disease severity, intensive care unit (ICU) admission, thromboembolism, and mortality[26]. Both C3 and C4 Levels were significantly lower in severe COVID-19 or deceased patients in a meta-analysis of 19 studies including 3764 patients[27]. Serum levels of C3 were reduced in the majority of a small cohort of healthcare workers with COVID-19, suggesting activation of the complement cascade and C3 consumption[28], while case series demonstrated that lower serum C3 on hospital admission or its progressive decline during hospitalization were associated with up to a 4-fold higher risk of disease progression[29,30]. Confirming these findings, Sinkovits *et al*[31] revealed an association between an increased C3a/C3 ratio and need for intubation/mechanical ventilation and in-hospital mortality, while Zhao *et al*[32] identified decreased C3 and C4 Levels in a cohort of 125 non-survivors hospitalized during the early stages of the pandemic in Wuhan. In contrast to the aforementioned findings, adjusted analysis in a cohort of 100 ICU patients including 81 patients with acute kidney injury demonstrated no association between kidney injury and the level of C3[33].

Dynamic changes of complement levels have been reported in patients with COVID-19. Alosaimi *et al*[34] reported higher C3a, C5a, and factor P (properdin) levels in severe COVID-19 that were also higher in critical COVID-19 non-survivors. Further, the levels were increased during the early stage and gradually decreased during hospital course. Continuous sampling in hemodialysis patients with severe COVID-19 identified that C5a levels were elevated prior to clinical deterioration. C3a levels remained elevated during the severe phase, whereas C5a levels started decreasing on day 7[35]. Interestingly, erythrocytes have been proposed as a diagnostic marker of disease progression based on the expression of complement receptors and complement binding. COVID-19 patients admitted to the ICU had an increased percentage of RBCs coated with C3b/iC3b/C3dg and C4d during the first 72 h of admission and the percentage increased further by day 7 in the study by Lam *et al*[36].

Complement component profiles were investigated by Defendi *et al*[37], who performed an extensive analysis of the functional activities and antigenic levels of individual complement components [C1q, C4, C3, C5, Factor B, and mannose-binding lectin (MBL)] and evaluated their association with clinical outcomes, including rate of ICU admission, corticosteroid treatment, oxygen requirement, and mortality. Two distinct profiles emerged: patients with greater disease severity and mortality exhibited activation of the lectin and alternative pathways and low levels of MBL, C4, C3, Factor B, and C5, while patients with more moderate disease showed inflammatory markers compatible with classical pathway activation.

Genetic polymorphisms of C3 have been identified and associated with COVID-19 susceptibility and mortality[38]. Gavriilaki *et al* used targeted next-generation sequencing and identified C3 variants as independent predictors of disease severity, ICU admission, and/or mortality, strengthening the hypothesis of genetic susceptibility in severe COVID-19[39,40]. Other genetic polymorphisms associated with severe disease include the mannose binding lectin gene 2 (rs1800450)[41,42] and the chromosome 3 rs11385942 G>GA variant that has been associated with complement overactivation (formation of C5a and MAC)[43].

Post-mortem histopathological studies of patients with severe COVID-19 revealed endothelial deposition of complement activation products in the lungs and skin, including C5b9, C3d, C4d, and the mannan-binding lectin serine protease 2 (MASP-2), an important mediator of the lectin pathway activation[9,44]. Similarly, Kim *et al*[45] identified immune complexes and MAC deposition in airways and vasculature of lung biopsies, enhanced viral antigen-specific responses in lung-derived myeloid cells, and significant increases in concentrations of C3a and C5a in critical COVID-19 patients. In a retrospective study of 74 patients with COVID-19, SARS-CoV-2 membrane and spike proteins and MASP-2 were also detected and co-localized in small bowel vessels of those patients with microvascular injury, supporting the role of thromboinflammation and complement activation[46]. Interestingly, binding of the SARS-CoV-2 spike protein S1 and S2 subunits to heparan sulfate on cell surfaces and binding of the S and N proteins to lectin pathway molecules cause excessive activation of the alternative and lectin pathways, respectively, resulting in end-organ damage[47,48]. In contrast to the lung and small bowel findings, Santana *et al*[49] reported a low rate of C4d deposition (22%) in liver histopathologic specimens of 27 deceased patients, suggesting that hepatocellular injury is a result of systemic

rather than intrahepatic thrombotic events.

THE ROLE OF COMPLEMENT IN COVID-19 INDUCED THROMBOTIC MICROANGIOPATHY

Coagulopathy resulting in a high frequency of thrombotic complications, including venous thromboembolism (VTE) such as deep vein thrombosis and pulmonary embolism, and arterial thromboembolism such as myocardial infarction and ischemic stroke, is common in critically ill COVID-19 patients and is among the leading causes of death[50,51]. The incidence of VTE has been estimated at 5.5% to 14.1% or more – an over two-fold higher risk compared to historical matched cohorts[52-54]. Microvascular thrombosis has been associated with progression to ARDS[55], while autopsy studies have identified VTE or *in situ* pulmonary arterial thrombosis in at least 60% of patients with COVID-19, suggesting thrombosis as a major cause of mortality[56,57].

The causal mechanisms of the COVID-19 coagulopathy are diverse and include dysregulated inflammation (cytokine storm) with subsequent activation of the coagulation cascade and platelets[50,58], virus induced endothelial changes[59-61], or patient comorbidities and limited mobility related to prolonged hospitalization[62]. Increased plasma levels of D-dimer, a marker of coagulation cascade activation, especially greater than 4 times the upper limit of normal, predict a more than two-fold increased risk of VTE or mortality[2,60], while thrombocytopenia and prothrombin time prolongation have also been observed[63].

In the context of thromboinflammation, the complement pathways are capable of activating the coagulation cascade through the induction of tissue factor expression[64,65]. Furthermore, serine proteases of the lectin pathway can cleave prothrombin to form activated thrombin, and MBL has been shown to be significantly increased in critically ill COVID-19 patients with symptomatic thromboembolism[66,67]. Complement system inhibitors, such as C1-esterase inhibitors, can additionally inhibit the coagulation cascade[68].

Current histopathologic data suggest TMA – manifesting as thrombocytopenia, microangiopathic hemolytic anemia, and organ damage – as a potential cause of severe COVID-19. TMA has been widely reported in postmortem studies, particularly as pulmonary capillary stasis and presence of microthrombi in the lungs, along with erythrocyte aggregation, endothelial injury, and fibrin thrombi in kidneys, despite anticoagulation[69,70].

Diffuse alveolar damage and complementmediated endothelial injury of septal microvasculature and microthrombi have been observed in critically ill patients with increased serum D-dimer levels and fibrinogendegradation products, further strengthening the concept of immunemediated pulmonary vascular injury and thrombosis in COVID-19[71]. Lung histopathologic data have also shown that severe COVID-19 is characterized by innate-immunity cell-mediated inflammatory endothelial damage manifesting as an obliterating endarteritis, associated with accumulation of C5aR1+ lung macrophages around the arteries and within thrombi[24,72]. This finding supports the notion that C5a production attracts and activates myeloid cells in the lungs, causing excessive inflammation and endothelial damage[24].

Complement-mediated renal TMA has been investigated in both adults and children with COVID-19, with evidence showing a constitutional complement dysregulation and intrarenal complement activation. These findings have been associated with genetic alterations of the alternative complement pathway and suggest SARS-CoV-2 as an emerging infectious trigger for atypical hemolytic uremic syndrome (aHUS), in accordance with previous cases precipitated by influenza strains[73]. COVID-19-associated renal TMA is characterized by increased deposition of complement components (C1q, C3, C5b9) and total immunoglobulin[74] and unrestrained formation of C5b9[75], which has also been observed in children with COVID-19 independent of disease severity and in the presence of clinical and diagnostic criteria of TMA[76]. Further confirming these findings, Cugno *et al*[77] identified an association between high levels of C5b9 levels and von-Willebrand factor and a positive association with disease severity, suggesting that complement activation and endothelial injury are major determinants of the clinical course of COVID-19 and potential treatment targets.

Cutaneous histopathologic data, derived from chilblain-like lesions, also known as "COVID toes" – inflammatory erythematous papules involving fingers and toes – are characterized by a significant transcriptomic activation of systemic immune response (type I IFN, IgA ANCA), complement activation (upregulation of C1q, C1s and C1 inhibitor, C2, properdin, and downregulation of MAC components C5 and C6), angiogenesis factors (VEGF-A, VEGFR-2 and c-Kit), and endothelial dysfunction (angiopoietin-1, angiopoietin-2 and VEGF-A)[78]. Skin findings may be associated with antiphospholipid antibodies as supported by an analysis of skin samples in a patient with severe COVID-19 with complement-induced vascular injury and severe thrombosis[79] and deposition of C5b9, MASP2, and C4d as shown by skin biopsies in three patients with treatment-resistant COVID-19[80].

Transcriptomic and proteomic analyses have provided important insights in the interaction between inflammation and coagulation pathways in COVID-19. Transcriptomic profiling of leukocytes from intensive care patients revealed the upregulated expression of genes involved in inflammation,

coagulation, and platelet function, concordant with the activation of complement pathways, including *SERPINE1* (plasminogen activator inhibitor-1; PAI-1), von Willebrand factor, and Granzyme B, factors involved in the Toll-like receptor-mediated cascades, and tumor necrosis factor/interleukin 6 (IL-6) signaling[81]. In order to further investigate the proteomic signature and identify biomarkers of disease severity in COVID-19, Barberis *et al*[82] conducted a proteomic profile characterization of plasma-derived exosomes from COVID-19 patients and healthy controls. They reported a specific proteomic signature of strongly regulated proteins in both critically and non-critically ill patients, compared to healthy subjects, including proteins involved in the acute phase response (C-reactive protein [CRP], serum amyloid A, and ferritin), immune-response (C1R, C4A/C4B, MBL2 and SERPING1), and coagulation (proteins of the intrinsic and extrinsic coagulation cascade, Kininogen-1), and reported that the C1r complement subcomponent is highly associated with disease severity, with an AUC of 0.93 (sensitivity: 89%; specificity: 82%). Consistent with the above findings, Freda *et al*[83] observed significant increases in thrombotic and inflammatory marker expression (thrombomodulin, PECAM-1) in human endothelial cells exposed to SARS-CoV-2 structural proteins. Kaiser *et al*[84] analyzed the proteome of neutrophils in severe COVID-19 and reported a unique proteomic signature of increased IL-8 secretion associated with increased D-dimer and neutrophil extracellular trap (NET) production, elevated complement factors (C1R, C1S, C5, C6, C7, C8 and C9), and fibrinogen binding, further uncovering a procoagulant role of inflammation and complement pathways. Lastly, NETs have been implicated in cytokine storm, and inhibition of C3aR and C5aR has been shown to attenuate thromboinflammation driven by NETs[75,85].

COMPLEMENT INHIBITION AS AN EFFECTIVE TARGET WITH THERAPEUTIC IMPLICATIONS

The complement system has garnered interest as a therapeutic target in the treatment of COVID-19. Several clinical trials investigating C1 esterase, C3, C5, C5a, or C5aR inhibition (Table 1) show reduced incidence of 28-d mortality and pulmonary embolism[86].

Most available evidence from case reports, small case series, and ongoing studies has focused on inhibition of C5, C5a, or C5aR. Eculizumab and ravulizumab are humanized monoclonal antibodies, currently used for the treatment of paroxysmal nocturnal hemoglobinuria (PNH) and aHUS, that bind to terminal complement component C5 with high affinity, preventing the subsequent formation of C5b9. C5 inhibition can attenuate hyperinflammatory lung damage caused by SARS-CoV-2 in PNH patients with active COVID-19 infection[87]. Those without underlying PNH or aHUS may also potentially derive benefit. In a case series of four patients with severe pneumonia or ARDS, patients received up to 4 infusions of eculizumab and showed a marked improvement in respiratory status and need for non-invasive ventilation within 48 h of the first dose and recovered completely[88]. Similarly, in eight patients with severe or critical COVID-19, six patients showed improved oxygenation after receiving a first dose of eculizumab and were ultimately discharged, while two patients died from septic shock and massive pulmonary embolism, respectively[22]. These findings were further reinforced by Zelek *et al*[89] who reported that Tesidolumab (LFG316), a C5-blocking monoclonal antibody, can rapidly decrease the hyperinflammatory response in 4 out of 5 critical patients with high levels of MAC not responding to standard treatment. Interestingly, in accordance with *in vivo* findings, *in vitro* C5aR inhibition in human airway epithelial cells results in epithelial integrity and promotes anti-inflammatory effects[90].

In patients with established TMA or PNH and concomitant COVID-19, the disease course was milder in those receiving eculizumab or ravulizumab[91,92]. In one of the largest studies (n = 80) of complement-targeted therapy in COVID-19, 35 ICU patients treated with eculizumab showed an improved 15-d survival of 82.9% (95%CI: 70.4%-95.3%) compared to 62.2% (95%CI: 48.1%-76.4%) without eculizumab, and improved 28-d survival of 80.0% (95%CI: 66.8%-93.3%) with eculizumab *vs* 51.1% (95%CI: 36.5%-65.7%) without eculizumab accompanied by reduction in key biomarkers (IL-6, IL-17, IFN a2 and C5b9)[93]. However, eculizumab administered in a regular schedule in the treatment of PNH was inadequate in the prevention of ARDS, raising questions regarding the optimal dose and administration in patients with severe COVID-19[94]. A combination of eculizumab with other immunomodulatory agents, such as ruxolitinib, a Janus Associated Kinase inhibitor, may result in improved outcomes and supports the hypothesis that the ideal treatment regimen may be multifaceted [95].

C3 inhibition is also under investigation as a potential therapeutic strategy. Genetic variants of the C3 protein can independently predict risk of developing severe COVID-19, need for ICU-level care, and mortality; this may provide a theoretical foundation for the early use of complement inhibitors[39]. The compstatin-based C3 inhibitor AMY-101 was safely and successfully used in a patient with SARS–CoV-2 associated pneumonia[96]. Further data from an exploratory study by Mastellos *et al*[97] in severe COVID-19 patients treated with eculizumab (n = 10) or AMY-101 (n = 3), showed attenuation of the hyperinflammatory response, especially with AMY-101. Both agents resulted in a significant decrease in inflammatory markers such as CRP and IL-6 and improved lung function. AMY-101 attenuated C3a and C5b9 levels, decreased fibrinogen consumption, neutrophil counts and NET formation, and enhanced

Table 1 Randomized clinical trials investigating complement inhibitors in the treatment of coronavirus disease 2019

NCT number	Drug	Mechanism of action	Status	Sponsor
NCT04395456	AMY-101	C3 inhibitor	Not yet recruiting	Amyndas Pharmaceuticals S.A.
NCT04402060	APL-9	C3 inhibitor	Completed	Apellis Pharmaceuticals, Inc.
NCT04346797	Eculizumab	C5 inhibitor	Recruiting	Assistance Publique- Hôpitaux de Paris
NCT04355494	Eculizumab	C5 inhibitor	Expanded access no longer available	Alexion Pharmaceuticals
NCT04288713	Eculizumab	C5 inhibitor	Expanded access available	Hudson Medical
NCT04351503	Eculizumab	C5 inhibitor	Recruiting	University Hospital, Basel, Switzerland
NCT04369469	Ravulizumab	C5 inhibitor	Terminated (Met futility bar at interim analysis)	Alexion Pharmaceuticals
NCT04382755	Zilucoplan (RA101495)	C5 inhibitor	Completed	University Hospital, Ghent
NCT04371367	Avdoralimab	Anti-C5aR	Completed	Assistance Publique Hopitaux De; Marseille &Innate Pharma
NCT04414631	Conestat alfa	C1 esterase inhibitors	Terminated	University Hospital, Basel, Switzerland & Pharming Technologies B.V.
NCT04530136	Ruconest	C1 esterase inhibitors	Recruiting	Pharming Technologies B.V.
NCT04333420	Vilobelimab (IFX-1)	C5a	Recruiting	InflaRx GmbH
NCT04570397	Ravulizumab	C5 inhibitor	Recruiting	Brigham and Women's Hospital
NCT04390464	Ravulizumab	C5 inhibitor	Recruiting	Cambridge University Hospitals NHS; Foundation Trust; Frances Hall

lymphocyte recovery.

The classical pathway has been targeted at the level of C1 esterase with inhibitors, such as Conestat alfa and Berinert, that have been previously used in patients with hereditary angioedema[98,99]. Berinert has similar anti-complement effects as heparin, which has demonstrated efficacy in COVID-19 treatment[100-102]. An exploratory study by Urwyler *et al*[103], which investigated Conestat alfa in 5 patients with severe COVID-19, showed improved clinical outcomes such as defervescence and recovery, and improved inflammatory markers levels including CRP, C4d and C5a. Common side effects for Conestat alfa and Berinert include nausea and vomiting alongside with other gastrointestinal symptoms and coinfections[104,105].

SARS-CoV-2 spike protein subunits 1 and 2 can directly activate the alternative pathway through interaction with heparan sulfate on host cell surfaces. This offers another potential therapeutic target as it could be prevented by small molecule inhibitors of factor D (ACH145951)[47]. These molecules bind factor D with high affinity and limit its proteolytic activity against proconvertase (Factor B in complex with C3b). Factor D deficiency is associated with increased risk for recurrent infections with encapsulated organisms comparable to other terminal complement deficiency syndromes[106].

The lectin pathway has been targeted with narsoplimab, an anti-MASP-2 monoclonal antibody, in the treatment of six critically ill or mechanically-ventilated patients, resulting in reduced endothelial damage and inflammation. Recipients showed an increased survival rate and improved inflammatory markers, including circulating endothelial cells, IL-6, IL-8, CRP, and LDH[107]. Common side effects include headache, upper respiratory infection, fatigue, nausea, vomiting, diarrhea, hypokalemia, neutropenia and fever[108,109]. A recently identified variant in the MBL gene 2 (rs1800450) has been associated with the need for hospitalization, severe disease, ICU admission, and development of pneumonia potentially suggesting a new therapeutic target[41,42].

Other potential targets include antibodies against SARS-CoV-2, such as nCoV396, a monoclonal antibody against the SARS-CoV-2 nucleocapsid (N) protein that has been shown to prevent the MASP-2-dependent complement activation. Binding of nCoV396 to the SARS-CoV 2 N protein leads to conformational changes that may lead to allosteric modulation of its protein function[110]. The precise interaction between the SARS-CoV-2 N protein and MASP2 remains under investigation. Overall, targeting N protein may be a feasible therapeutic strategy.

Given the fact that only a small proportion of patients will develop aggressive disease, reliable clinical indicators to identify these patients in the early phase of disease progression are of utmost importance. The time window for optimal intervention and the patient populations that could benefit from therapeutic complement inhibition have yet to be determined. Currently available biomarkers of complement activity are too unstable and short-lived to be used predictively. Nevertheless, clinical

predictors of ARDS progression combined with inflammatory biomarkers (CRP, IL-6, ferritin, and D-dimer) could potentially allow the identification of patients that could benefit from early intervention[2,111].

Theoretically, upstream targets in the complement pathway would provide the most potent anti-inflammatory results[96]. Despite the fact that the use of anti-C5a antibodies has been associated with prominent clinical improvement and decreased systemic inflammation, C5 inhibition can be partial, allowing residual terminal pathway activity in cases of excessive complement activation, as seen in severe COVID-19. In these advanced stages of COVID-19, C3 inhibition has the ability to control both ARDS and the systemic inflammation that damages the microcirculation of vital organs. Proximal complement inhibitors which target C3 or its upstream activators are appealing targets, but their benefit in mortality was not confirmed in a randomized, double-blinded, multicenter study that compared APL-9 (C3 inhibitor) to standard of care in mild to moderate COVID-19[112]. Further randomized studies comparing different complement inhibitors are necessary to identify the most appropriate therapeutic agents, as well as the benefits of upstream inhibition or pathway specific targeting.

The available data should be interpreted with caution. Concurrent use of antiviral drugs, corticosteroids, heparin, and antibiotics in these studies significantly limits their generalizability. The increased risk of opportunistic infections, most notoriously with encapsulated organisms (*Neisseria*, *Haemophilus*, or *Streptococcus* species) in unvaccinated individuals and those with asplenia or functional asplenia, through the inhibition of terminal complement proteins has historically limited complement inhibitor use. However, growing clinical experience with C5-inhibitors and C3-inhibitors such as APL-2 and AMY-101/Cp40 along with prophylactic antibiotics or planned vaccination schedules has assuaged these concerns. Additionally, individualized treatment strategies based on specific immunologic profiles and complement-driven disease should be further investigated[113].

The complement system can also be theoretically exploited alongside the use of COVID-19 vaccines and antibody-based therapies. Complement activation is known to enhance the efficacy of pathogen-neutralizing antibodies through formation of larger antibody-C1q complexes, and thus may require fewer IgG molecules bound to virus surfaces to facilitate their neutralization[114,115]. Monoclonal antibodies or vaccines can potentially be engineered to promote enhanced C1q binding and complement activation leading to a more robust immunologic response, confronting the problem of waning antibody concentrations with traditional immunization approaches[115,116]. The risk of vaccine-induced thrombotic thrombocytopenia seen with the use of COVID-19 adenovirus-vector vaccines that is thought to be mediated by anti-platelet factor 4 antibodies and subsequent complement activation remains a concern[117]. Thus, a careful weighing of risks is essential.

CONCLUSION

Current evidence suggests excessive complement activation and subsequent complement-dependent cytotoxic tissue damage drives COVID-19 progression and thromboembolic complications. In the context of thromboinflammation, the three complement pathways can activate the coagulation cascade causing TMA and end-organ damage, mostly manifesting as lung, kidney, and cutaneous disease. Considering its role in cytokine storm and thrombogenesis, the complement system is an appealing treatment target. Preliminary reports have produced promising results. Whether inhibition of upstream (C3, C1) or terminal (C5, C5a, or C5aR) components is of greater importance remains to be elucidated. Current data indicate the need for evaluation of complement inhibitors as COVID-19 therapeutics, and many are under investigation in prospective randomized trials. Limitations such as the cost of inhibitors or their association with opportunistic infections may preclude their generalized use in the treatment of COVID-19.

ACKNOWLEDGEMENTS

Access to Biorender.com and publishing rights of Figure 1 were kindly provided by Dr. Georgios Geropoulos, who had access on a paid subscription.

FOOTNOTES

Author contributions: Gianni P, and Giannis D led the study including review of the literature, data analysis, and drafted the manuscript; Goldin M, Ngu S, Geropoulos G and Zafeiropoulos S contributed to the editing, data analysis and critical review of the manuscript; all authors are agreeable to be accountable for all aspects of the work and gave final approval of the version to be published.

Conflict-of-interest statement: All the authors declare no conflict of interests for this article.

Country/Territory of origin: United States

ORCID number: Panagiota Gianni 0000-0001-9246-1234; Mark Goldin 0000-0002-1147-5541; Sam Ngu 0000-0002-2256-067X; Stefanos Zafeiropoulos 0000-0002-3284-2515; Georgios Geropoulos 0000-0002-2066-7975; Dimitrios Giannis 0000-0001-9246-976X.

S-Editor: Liu JH
L-Editor: A
P-Editor: Liu JH

REFERENCES

1 **Wang D**, Hu B, Hu C, Zhu F, Liu X, Zhang J, Wang B, Xiang H, Cheng Z, Xiong Y, Zhao Y, Li Y, Wang X, Peng Z. Clinical Characteristics of 138 Hospitalized Patients With 2019 Novel Coronavirus-Infected Pneumonia in Wuhan, China. *JAMA* 2020; **323**: 1061-1069 [PMID: 32031570 DOI: 10.1001/jama.2020.1585]
2 **Cohen SL**, Gianos E, Barish MA, Chatterjee S, Kohn N, Lesser M, Giannis D, Coppa K, Hirsch JS, McGinn TG, Goldin ME, Spyropoulos AC; Northwell Health COVID-19 Research Consortium. Prevalence and Predictors of Venous Thromboembolism or Mortality in Hospitalized COVID-19 Patients. *Thromb Haemost* 2021; **121**: 1043-1053 [PMID: 33472255 DOI: 10.1055/a-1366-9656]
3 **Li X**, Ma X. Acute respiratory failure in COVID-19: is it "typical" ARDS? *Crit Care* 2020; **24**: 198 [PMID: 32375845 DOI: 10.1186/s13054-020-02911-9]
4 **Coperchini F**, Chiovato L, Croce L, Magri F, Rotondi M. The cytokine storm in COVID-19: An overview of the involvement of the chemokine/chemokine-receptor system. *Cytokine Growth Factor Rev* 2020; **53**: 25-32 [PMID: 32446778 DOI: 10.1016/j.cytogfr.2020.05.003]
5 **Chen G**, Wu D, Guo W, Cao Y, Huang D, Wang H, Wang T, Zhang X, Chen H, Yu H, Zhang M, Wu S, Song J, Chen T, Han M, Li S, Luo X, Zhao J, Ning Q. Clinical and immunological features of severe and moderate coronavirus disease 2019. *J Clin Invest* 2020; **130**: 2620-2629 [PMID: 32217835 DOI: 10.1172/JCI137244]
6 **Xu X**, Han M, Li T, Sun W, Wang D, Fu B, Zhou Y, Zheng X, Yang Y, Li X, Zhang X, Pan A, Wei H. Effective treatment of severe COVID-19 patients with tocilizumab. *Proc Natl Acad Sci U S A* 2020; **117**: 10970-10975 [PMID: 32350134 DOI: 10.1073/pnas.2005615117]
7 **Fajgenbaum DC**, June CH. Cytokine Storm. *N Engl J Med* 2020; **383**: 2255-2273 [PMID: 33264547 DOI: 10.1056/NEJMra2026131]
8 **Keshavarz F**, Ghalamfarsa F, Javdansirat S, Hasanzadeh S, Azizi A, Sabz G, Salehi M, Ghalamfarsa G. Patients with Covid 19 have significantly reduced CH50 activity. *Virusdisease* 2021; 1-9 [PMID: 34631971 DOI: 10.1007/s13337-021-00710-6]
9 **Magro C**, Mulvey JJ, Berlin D, Nuovo G, Salvatore S, Harp J, Baxter-Stoltzfus A, Laurence J. Complement associated microvascular injury and thrombosis in the pathogenesis of severe COVID-19 infection: A report of five cases. *Transl Res* 2020; **220**: 1-13 [PMID: 32299776 DOI: 10.1016/j.trsl.2020.04.007]
10 **Shen B**, Yi X, Sun Y, Bi X, Du J, Zhang C, Quan S, Zhang F, Sun R, Qian L, Ge W, Liu W, Liang S, Chen H, Zhang Y, Li J, Xu J, He Z, Chen B, Wang J, Yan H, Zheng Y, Wang D, Zhu J, Kong Z, Kang Z, Liang X, Ding X, Ruan G, Xiang N, Cai X, Gao H, Li L, Li S, Xiao Q, Lu T, Zhu Y, Liu H, Guo T. Proteomic and Metabolomic Characterization of COVID-19 Patient Sera. *Cell* 2020; **182**: 59-72.e15 [PMID: 32492406 DOI: 10.1016/j.cell.2020.05.032]
11 **Mellors J**, Tipton T, Longet S, Carroll M. Viral Evasion of the Complement System and Its Importance for Vaccines and Therapeutics. *Front Immunol* 2020; **11**: 1450 [PMID: 32733480 DOI: 10.3389/fimmu.2020.01450]
12 **Pandya PH**, Wilkes DS. Complement system in lung disease. *Am J Respir Cell Mol Biol* 2014; **51**: 467-473 [PMID: 24901241 DOI: 10.1165/rcmb.2013-0485TR]
13 **Barrington RA**, Schneider TJ, Pitcher LA, Mempel TR, Ma M, Barteneva NS, Carroll MC. Uncoupling CD21 and CD19 of the B-cell coreceptor. *Proc Natl Acad Sci U S A* 2009; **106**: 14490-14495 [PMID: 19706534 DOI: 10.1073/pnas.0903477106]
14 **Wang R**, Xiao H, Guo R, Li Y, Shen B. The role of C5a in acute lung injury induced by highly pathogenic viral infections. *Emerg Microbes Infect* 2015; **4**: e28 [PMID: 26060601 DOI: 10.1038/emi.2015.28]
15 **Bjornson AB**, Mellencamp MA, Schiff GM. Complement is activated in the upper respiratory tract during influenza virus infection. *Am Rev Respir Dis* 1991; **143**: 1062-1066 [PMID: 2024815 DOI: 10.1164/ajrccm/143.5_Pt_1.1062]
16 **Ohta R**, Torii Y, Imai M, Kimura H, Okada N, Ito Y. Serum concentrations of complement anaphylatoxins and proinflammatory mediators in patients with 2009 H1N1 influenza. *Microbiol Immunol* 2011; **55**: 191-198 [PMID: 21244468 DOI: 10.1111/j.1348-0421.2011.00309.x]
17 **Gralinski LE**, Sheahan TP, Morrison TE, Menachery VD, Jensen K, Leist SR, Whitmore A, Heise MT, Baric RS. Complement Activation Contributes to Severe Acute Respiratory Syndrome Coronavirus Pathogenesis. *mBio* 2018; **9** [PMID: 30301856 DOI: 10.1128/mBio.01753-18]

18 **Sun S**, Zhao G, Liu C, Wu X, Guo Y, Yu H, Song H, Du L, Jiang S, Guo R, Tomlinson S, Zhou Y. Inhibition of complement activation alleviates acute lung injury induced by highly pathogenic avian influenza H5N1 virus infection. *Am J Respir Cell Mol Biol* 2013; **49**: 221-230 [PMID: 23526211 DOI: 10.1165/rcmb.2012-0428OC]

19 **Jiang Y**, Zhao G, Song N, Li P, Chen Y, Guo Y, Li J, Du L, Jiang S, Guo R, Sun S, Zhou Y. Blockade of the C5a-C5aR axis alleviates lung damage in hDPP4-transgenic mice infected with MERS-CoV. *Emerg Microbes Infect* 2018; **7**: 77 [PMID: 29691378 DOI: 10.1038/s41426-018-0063-8]

20 **Sun S**, Zhao G, Liu C, Fan W, Zhou X, Zeng L, Guo Y, Kou Z, Yu H, Li J, Wang R, Li Y, Schneider C, Habel M, Riedemann NC, Du L, Jiang S, Guo R, Zhou Y. Treatment with anti-C5a antibody improves the outcome of H7N9 virus infection in African green monkeys. *Clin Infect Dis* 2015; **60**: 586-595 [PMID: 25433014 DOI: 10.1093/cid/ciu887]

21 **Fernández S**, Moreno-Castaño AB, Palomo M, Martinez-Sanchez J, Torramadé-Moix S, Téllez A, Ventosa H, Seguí F, Escolar G, Carreras E, Nicolás JM, Richardson E, García-Bernal D, Carlo-Stella C, Moraleda JM, Richardson PG, Díaz-Ricart M, Castro P. Distinctive Biomarker Features in the Endotheliopathy of COVID-19 and Septic Syndromes. *Shock* 2022; **57**: 95-105 [PMID: 34172614 DOI: 10.1097/SHK.0000000000001823]

22 **Peffault de Latour R**, Bergeron A, Lengline E, Dupont T, Marchal A, Galicier L, de Castro N, Bondeelle L, Darmon M, Dupin C, Dumas G, Leguen P, Madelaine I, Chevret S, Molina JM, Azoulay E, Fremeaux-Bacchi V; Core Group. Complement C5 inhibition in patients with COVID-19 - a promising target? *Haematologica* 2020; **105**: 2847-2850 [PMID: 33256385 DOI: 10.3324/haematol.2020.260117]

23 **Yu J**, Gerber GF, Chen H, Yuan X, Chaturvedi S, Braunstein EM, Brodsky RA. Complement dysregulation is associated with severe COVID-19 illness. *Haematologica* 2022; **107**: 1095-1105 [PMID: 34289657 DOI: 10.3324/haematol.2021.279155]

24 **Carvelli J**, Demaria O, Vély F, Batista L, Chouaki Benmansour N, Fares J, Carpentier S, Thibult ML, Morel A, Remark R, André P, Represa A, Piperoglou C; Explore COVID-19 IPH group; Explore COVID-19 Marseille Immunopole group, Cordier PY, Le Dault E, Guervilly C, Simeone P, Gainnier M, Morel Y, Ebbo M, Schleinitz N, Vivier E. Association of COVID-19 inflammation with activation of the C5a-C5aR1 axis. *Nature* 2020; **588**: 146-150 [PMID: 32726800 DOI: 10.1038/s41586-020-2600-6]

25 **Holter JC**, Pischke SE, de Boer E, Lind A, Jenum S, Holten AR, Tonby K, Barratt-Due A, Sokolova M, Schjalm C, Chaban V, Kolderup A, Tran T, Tollefsrud Gjølberg T, Skeie LG, Hesstvedt L, Ormåsen V, Fevang B, Austad C, Müller KE, Fladeby C, Holberg-Petersen M, Halvorsen B, Müller F, Aukrust P, Dudman S, Ueland T, Andersen JT, Lund-Johansen F, Heggelund L, Dyrhol-Riise AM, Mollnes TE. Systemic complement activation is associated with respiratory failure in COVID-19 hospitalized patients. *Proc Natl Acad Sci U S A* 2020; **117**: 25018-25025 [PMID: 32943538 DOI: 10.1073/pnas.2010540117]

26 **de Nooijer AH**, Grondman I, Janssen NAF, Netea MG, Willems L, van de Veerdonk FL, Giamarellos-Bourboulis EJ, Toonen EJM, Joosten LAB; RCI-COVID-19 study group. Complement Activation in the Disease Course of Coronavirus Disease 2019 and Its Effects on Clinical Outcomes. *J Infect Dis* 2021; **223**: 214-224 [PMID: 33038254 DOI: 10.1093/infdis/jiaa646]

27 **Zinellu A**, Mangoni AA. Serum Complement C3 and C4 and COVID-19 Severity and Mortality: A Systematic Review and Meta-Analysis With Meta-Regression. *Front Immunol* 2021; **12**: 696085 [PMID: 34163491 DOI: 10.3389/fimmu.2021.696085]

28 **Wei XS**, Wang XR, Zhang JC, Yang WB, Ma WL, Yang BH, Jiang NC, Gao ZC, Shi HZ, Zhou Q. A cluster of health care workers with COVID-19 pneumonia caused by SARS-CoV-2. *J Microbiol Immunol Infect* 2021; **54**: 54-60 [PMID: 32359943 DOI: 10.1016/j.jmii.2020.04.013]

29 **Jiang H**, Chen Q, Zheng S, Guo C, Luo J, Wang H, Zheng X, Weng Z. Association of Complement C3 with Clinical Deterioration Among Hospitalized Patients with COVID-19. *Int J Gen Med* 2022; **15**: 849-857 [PMID: 35115811 DOI: 10.2147/IJGM.S348519]

30 **Fang S**, Wang H, Lu L, Jia Y, Xia Z. Decreased complement C3 levels are associated with poor prognosis in patients with COVID-19: A retrospective cohort study. *Int Immunopharmacol* 2020; **89**: 107070 [PMID: 33039965 DOI: 10.1016/j.intimp.2020.107070]

31 **Sinkovits G**, Réti M, Müller V, Iványi Z, Gál J, Gopcsa L, Reményi P, Szathmáry B, Lakatos B, Szlávik J, Bobek I, Prohászka ZZ, Förhécz Z, Mező B, Csuka D, Hurler L, Kajdácsi E, Cervenak L, Kiszel P, Masszi T, Vályi-Nagy I, Prohászka Z. Associations between the von Willebrand Factor-ADAMTS13 Axis, Complement Activation, and COVID-19 Severity and Mortality. *Thromb Haemost* 2022; **122**: 240-256 [PMID: 35062036 DOI: 10.1055/s-0041-1740182]

32 **Zhao Y**, Nie HX, Hu K, Wu XJ, Zhang YT, Wang MM, Wang T, Zheng ZS, Li XC, Zeng SL. Abnormal immunity of non-survivors with COVID-19: predictors for mortality. *Infect Dis Poverty* 2020; **9**: 108 [PMID: 32746940 DOI: 10.1186/s40249-020-00723-1]

33 **Joseph A**, Zafrani L, Mabrouki A, Azoulay E, Darmon M. Acute kidney injury in patients with SARS-CoV-2 infection. *Ann Intensive Care* 2020; **10**: 117 [PMID: 32880774 DOI: 10.1186/s13613-020-00734-z]

34 **Alosaimi B**, Mubarak A, Hamed ME, Almutairi AZ, Alrashed AA, AlJuryyan A, Enani M, Alenzi FQ, Alturaiki W. Complement Anaphylatoxins and Inflammatory Cytokines as Prognostic Markers for COVID-19 Severity and In-Hospital Mortality. *Front Immunol* 2021; **12**: 668725 [PMID: 34276659 DOI: 10.3389/fimmu.2021.668725]

35 **Prendecki M**, Clarke C, Medjeral-Thomas N, McAdoo SP, Sandhu E, Peters JE, Thomas DC, Willicombe M, Botto M, Pickering MC. Temporal changes in complement activation in haemodialysis patients with COVID-19 as a predictor of disease progression. *Clin Kidney J* 2020; **13**: 889-896 [PMID: 33123364 DOI: 10.1093/ckj/sfaa192]

36 **Lam LKM**, Reilly JP, Rux AH, Murphy SJ, Kuri-Cervantes L, Weisman AR, Ittner CAG, Pampena MB, Betts MR, Wherry EJ, Song WC, Lambris JD, Meyer NJ, Cines DB, Mangalmurti NS. Erythrocytes identify complement activation in patients with COVID-19. *Am J Physiol Lung Cell Mol Physiol* 2021; **321**: L485-L489 [PMID: 34231390 DOI: 10.1152/ajplung.00231.2021]

37 **Defendi F**, Leroy C, Epaulard O, Clavarino G, Vilotitch A, Le Marechal M, Jacob MC, Raskovalova T, Pernollet M, Le Gouellec A, Bosson JL, Poignard P, Roustit M, Thielens N, Dumestre-Pérard C, Cesbron JY. Complement Alternative and Mannose-Binding Lectin Pathway Activation Is Associated With COVID-19 Mortality. *Front Immunol* 2021; **12**: 742446

[PMID: 34567008 DOI: 10.3389/fimmu.2021.742446]

38 **Delanghe JR**, De Buyzere ML, Speeckaert MM. Genetic Polymorphisms in the Host and COVID-19 Infection. *Adv Exp Med Biol* 2021; **1318**: 109-118 [PMID: 33973175 DOI: 10.1007/978-3-030-63761-3_7]

39 **Gavriilaki E**, Asteris PG, Touloumenidou T, Koravou EE, Koutra M, Papayanni PG, Karali V, Papalexandri A, Varelas C, Chatzopoulou F, Chatzidimitriou M, Chatzidimitriou D, Veleni A, Grigoriadis S, Rapti E, Chloros D, Kioumis I, Kaimakamis E, Bitzani M, Boumpas D, Tsantes A, Sotiropoulos D, Sakellari I, Kalantzis IG, Parastatidis ST, Koopialipoor M, Cavaleri L, Armaghani DJ, Papadopoulou A, Brodsky RA, Kokoris S, Anagnostopoulos A. Genetic justification of severe COVID-19 using a rigorous algorithm. *Clin Immunol* 2021; **226**: 108726 [PMID: 33845193 DOI: 10.1016/j.clim.2021.108726]

40 **Asteris PG**, Gavriilaki E, Touloumenidou T, Koravou EE, Koutra M, Papayanni PG, Pouleres A, Karali V, Lemonis ME, Mamou A, Skentou AD, Papalexandri A, Varelas C, Chatzopoulou F, Chatzidimitriou M, Chatzidimitriou D, Veleni A, Rapti E, Kioumis I, Kaimakamis E, Bitzani M, Boumpas D, Tsantes A, Sotiropoulos D, Papadopoulou A, Kalantzis IG, Vallianatou LA, Armaghani DJ, Cavaleri L, Gandomi AH, Hajihassani M, Hasanipanah M, Koopialipoor M, Lourenço PB, Samui P, Zhou J, Sakellari I, Valsami S, Politou M, Kokoris S, Anagnostopoulos A. Genetic prediction of ICU hospitalization and mortality in COVID-19 patients using artificial neural networks. *J Cell Mol Med* 2022; **26**: 1445-1455 [PMID: 35064759 DOI: 10.1111/jcmm.17098]

41 **Speletas M**, Dadouli K, Syrakouli A, Gatselis N, Germanidis G, Mouchtouri VA, Koulas I, Samakidou A, Nikolaidou A, Stefos A, Mimtsoudis I, Hatzianastasiou S, Koureas M, Anagnostopoulos L, Tseroni M, Tsinti G, Metallidis S, Dalekos G, Hadjichristodoulou C. MBL deficiency-causing B allele (rs1800450) as a risk factor for severe COVID-19. *Immunobiology* 2021; **226**: 152136 [PMID: 34628288 DOI: 10.1016/j.imbio.2021.152136]

42 **Medetalibeyoglu A**, Bahat G, Senkal N, Kose M, Avci K, Sayin GY, Isoglu-Alkac U, Tukek T, Pehlivan S. Mannose binding lectin gene 2 (rs1800450) missense variant may contribute to development and severity of COVID-19 infection. *Infect Genet Evol* 2021; **89**: 104717 [PMID: 33515713 DOI: 10.1016/j.meegid.2021.104717]

43 **Valenti L**, Griffini S, Lamorte G, Grovetti E, Uceda Renteria SC, Malvestiti F, Scudeller L, Bandera A, Peyvandi F, Prati D, Meroni P, Cugno M. Chromosome 3 cluster rs11385942 variant links complement activation with severe COVID-19. *J Autoimmun* 2021; **117**: 102595 [PMID: 33453462 DOI: 10.1016/j.jaut.2021.102595]

44 **Macor P**, Durigutto P, Mangogna A, Bussani R, De Maso L, D'Errico S, Zanon M, Pozzi N, Meroni PL, Tedesco F. Multiple-Organ Complement Deposition on Vascular Endothelium in COVID-19 Patients. *Biomedicines* 2021; **9** [PMID: 34440207 DOI: 10.3390/biomedicines9081003]

45 **Kim DM**, Kim Y, Seo JW, Lee J, Park U, Ha NY, Koh J, Park H, Lee JW, Ro HJ, Yun NR, Kim DY, Yoon SH, Na YS, Moon DS, Lim SC, Kim CM, Jeon K, Kang JG, Jang NY, Jeong H, Kim J, Cheon S, Sohn KM, Moon JY, Kym S, Han SR, Lee MS, Kim HJ, Park WY, Choi JY, Shin HW, Kim HY, Cho CH, Jeon YK, Kim YS, Cho NH. Enhanced eosinophil-mediated inflammation associated with antibody and complement-dependent pneumonic insults in critical COVID-19. *Cell Rep* 2021; **37**: 109798 [PMID: 34587481 DOI: 10.1016/j.celrep.2021.109798]

46 **Plotz B**, Castillo R, Melamed J, Magro C, Rosenthal P, Belmont HM. Focal small bowel thrombotic microvascular injury in COVID-19 mediated by the lectin complement pathway masquerading as lupus enteritis. *Rheumatology (Oxford)* 2021; **60**: e61-e63 [PMID: 33147605 DOI: 10.1093/rheumatology/keaa627]

47 **Yu J**, Yuan X, Chen H, Chaturvedi S, Braunstein EM, Brodsky RA. Direct activation of the alternative complement pathway by SARS-CoV-2 spike proteins is blocked by factor D inhibition. *Blood* 2020; **136**: 2080-2089 [PMID: 32877502 DOI: 10.1182/blood.2020008248]

48 **Ali YM**, Ferrari M, Lynch NJ, Yaseen S, Dudler T, Gragerov S, Demopulos G, Heeney JL, Schwaeble WJ. Lectin Pathway Mediates Complement Activation by SARS-CoV-2 Proteins. *Front Immunol* 2021; **12**: 714511 [PMID: 34290717 DOI: 10.3389/fimmu.2021.714511]

49 **Santana MF**, Guerra MT, Hundt MA, Ciarleglio MM, Pinto RAA, Dutra BG, Xavier MS, Lacerda MVG, Ferreira AJ, Wanderley DC, Borges do Nascimento IJ, Araújo RFA, Pinheiro SVB, Araújo SA, Leite MF, Ferreira LCL, Nathanson MH, Vieira Teixeira Vidigal P. Correlation Between Clinical and Pathological Findings of Liver Injury in 27 Patients With Lethal COVID-19 Infections in Brazil. *Hepatol Commun* 2022; **6**: 270-280 [PMID: 34520633 DOI: 10.1002/hep4.1820]

50 **Giannis D**, Ziogas IA, Gianni P. Coagulation disorders in coronavirus infected patients: COVID-19, SARS-CoV-1, MERS-CoV and lessons from the past. *J Clin Virol* 2020; **127**: 104362 [PMID: 32305883 DOI: 10.1016/j.jcv.2020.104362]

51 **Spyropoulos AC**, Levy JH, Ageno W, Connors JM, Hunt BJ, Iba T, Levi M, Samama CM, Thachil J, Giannis D, Douketis JD; Subcommittee on Perioperative, Critical Care Thrombosis, Haemostasis of the Scientific, Standardization Committee of the International Society on Thrombosis and Haemostasis. Scientific and Standardization Committee communication: Clinical guidance on the diagnosis, prevention, and treatment of venous thromboembolism in hospitalized patients with COVID-19. *J Thromb Haemost* 2020; **18**: 1859-1865 [PMID: 32459046 DOI: 10.1111/jth.14929]

52 **Klok FA**, Kruip MJHA, van der Meer NJM, Arbous MS, Gommers D, Kant KM, Kaptein FHJ, van Paassen J, Stals MAM, Huisman MV, Endeman H. Confirmation of the high cumulative incidence of thrombotic complications in critically ill ICU patients with COVID-19: An updated analysis. *Thromb Res* 2020; **191**: 148-150 [PMID: 32381264 DOI: 10.1016/j.thromres.2020.04.041]

53 **Nopp S**, Moik F, Jilma B, Pabinger I, Ay C. Risk of venous thromboembolism in patients with COVID-19: A systematic review and meta-analysis. *Res Pract Thromb Haemost* 2020 [PMID: 33043231 DOI: 10.1002/rth2.12439]

54 **Poissy J**, Goutay J, Caplan M, Parmentier E, Duburcq T, Lassalle F, Jeanpierre E, Rauch A, Labreuche J, Susen S; Lille ICU Haemostasis COVID-19 Group. Pulmonary Embolism in Patients With COVID-19: Awareness of an Increased Prevalence. *Circulation* 2020; **142**: 184-186 [PMID: 32330083 DOI: 10.1161/CIRCULATIONAHA.120.047430]

55 **Berger JS**, Connors JM. Anticoagulation in COVID-19: reaction to the ACTION trial. *Lancet* 2021; **397**: 2226-2228 [PMID: 34119049 DOI: 10.1016/S0140-6736(21)01291-5]

56 **Lax SF**, Skok K, Zechner P, Kessler HH, Kaufmann N, Koelblinger C, Vander K, Bargfrieder U, Trauner M. Pulmonary Arterial Thrombosis in COVID-19 With Fatal Outcome : Results From a Prospective, Single-Center, Clinicopathologic

Case Series. *Ann Intern Med* 2020; **173**: 350-361 [PMID: 32422076 DOI: 10.7326/M20-2566]

57 **Wichmann D**, Sperhake JP, Lütgehetmann M, Steurer S, Edler C, Heinemann A, Heinrich F, Mushumba H, Kniep I, Schröder AS, Burdelski C, de Heer G, Nierhaus A, Frings D, Pfefferle S, Becker H, Bredereke-Wiedling H, de Weerth A, Paschen HR, Sheikhzadeh-Eggers S, Stang A, Schmiedel S, Bokemeyer C, Addo MM, Aepfelbacher M, Püschel K, Kluge S. Autopsy Findings and Venous Thromboembolism in Patients With COVID-19: A Prospective Cohort Study. *Ann Intern Med* 2020; **173**: 268-277 [PMID: 32374815 DOI: 10.7326/M20-2003]

58 **Spyropoulos AC**, Weitz JI. Hospitalized COVID-19 Patients and Venous Thromboembolism: A Perfect Storm. *Circulation* 2020; **142**: 129-132 [PMID: 32658609 DOI: 10.1161/CIRCULATIONAHA.120.048020]

59 **Bikdeli B**, Madhavan MV, Jimenez D, Chuich T, Dreyfus I, Driggin E, Nigoghossian C, Ageno W, Madjid M, Guo Y, Tang LV, Hu Y, Giri J, Cushman M, Quéré I, Dimakakos EP, Gibson CM, Lippi G, Favaloro EJ, Fareed J, Caprini JA, Tafur AJ, Burton JR, Francese DP, Wang EY, Falanga A, McLintock C, Hunt BJ, Spyropoulos AC, Barnes GD, Eikelboom JW, Weinberg I, Schulman S, Carrier M, Piazza G, Beckman JA, Steg PG, Stone GW, Rosenkranz S, Goldhaber SZ, Parikh SA, Monreal M, Krumholz HM, Konstantinides SV, Weitz JI, Lip GYH; Global COVID-19 Thrombosis Collaborative Group, Endorsed by the ISTH, NATF, ESVM, and the IUA, Supported by the ESC Working Group on Pulmonary Circulation and Right Ventricular Function. COVID-19 and Thrombotic or Thromboembolic Disease: Implications for Prevention, Antithrombotic Therapy, and Follow-Up: JACC State-of-the-Art Review. *J Am Coll Cardiol* 2020; **75**: 2950-2973 [PMID: 32311448 DOI: 10.1016/j.jacc.2020.04.031]

60 **Tang N**, Li D, Wang X, Sun Z. Abnormal coagulation parameters are associated with poor prognosis in patients with novel coronavirus pneumonia. *J Thromb Haemost* 2020; **18**: 844-847 [PMID: 32073213 DOI: 10.1111/jth.14768]

61 **Iba T**, Levy JH, Levi M, Connors JM, Thachil J. Coagulopathy of Coronavirus Disease 2019. *Crit Care Med* 2020; **48**: 1358-1364 [PMID: 32467443 DOI: 10.1097/CCM.0000000000004458]

62 **Zhang Y**, Xiao M, Zhang S, Xia P, Cao W, Jiang W, Chen H, Ding X, Zhao H, Zhang H, Wang C, Zhao J, Sun X, Tian R, Wu W, Wu D, Ma J, Chen Y, Zhang D, Xie J, Yan X, Zhou X, Liu Z, Wang J, Du B, Qin Y, Gao P, Qin X, Xu Y, Zhang W, Li T, Zhang F, Zhao Y, Li Y. Coagulopathy and Antiphospholipid Antibodies in Patients with Covid-19. *N Engl J Med* 2020; **382**: e38 [PMID: 32268022 DOI: 10.1056/NEJMc2007575]

63 **Zhou F**, Yu T, Du R, Fan G, Liu Y, Liu Z, Xiang J, Wang Y, Song B, Gu X, Guan L, Wei Y, Li H, Wu X, Xu J, Tu S, Zhang Y, Chen H, Cao B. Clinical course and risk factors for mortality of adult inpatients with COVID-19 in Wuhan, China: a retrospective cohort study. *Lancet* 2020; **395**: 1054-1062 [PMID: 32171076 DOI: 10.1016/S0140-6736(20)30566-3]

64 **Wojta J**, Huber K, Valent P. New aspects in thrombotic research: complement induced switch in mast cells from a profibrinolytic to a prothrombotic phenotype. *Pathophysiol Haemost Thromb* 2003; **33**: 438-441 [PMID: 15692257 DOI: 10.1159/000083842]

65 **Tiwari R**, Mishra AR, Mikaeloff F, Gupta S, Mirazimi A, Byrareddy SN, Neogi U, Nayak D. *In silico* and *in vitro* studies reveal complement system drives coagulation cascade in SARS-CoV-2 pathogenesis. *Comput Struct Biotechnol J* 2020; **18**: 3734-3744 [PMID: 33200027 DOI: 10.1016/j.csbj.2020.11.005]

66 **Krarup A**, Wallis R, Presanis JS, Gál P, Sim RB. Simultaneous activation of complement and coagulation by MBL-associated serine protease 2. *PLoS One* 2007; **2**: e623 [PMID: 17637839 DOI: 10.1371/journal.pone.0000623]

67 **Eriksson O**, Hultström M, Persson B, Lipcsey M, Ekdahl KN, Nilsson B, Frithiof R. Mannose-Binding Lectin is Associated with Thrombosis and Coagulopathy in Critically Ill COVID-19 Patients. *Thromb Haemost* 2020; **120**: 1720-1724 [PMID: 32871607 DOI: 10.1055/s-0040-1715835]

68 **Davis AE 3rd**. Biological effects of C1 inhibitor. *Drug News Perspect* 2004; **17**: 439-446 [PMID: 15514703 DOI: 10.1358/dnp.2004.17.7.863703]

69 **Menter T**, Haslbauer JD, Nienhold R, Savic S, Hopfer H, Deigendesch N, Frank S, Turek D, Willi N, Pargger H, Bassetti S, Leuppi JD, Cathomas G, Tolnay M, Mertz KD, Tzankov A. Postmortem examination of COVID-19 patients reveals diffuse alveolar damage with severe capillary congestion and variegated findings in lungs and other organs suggesting vascular dysfunction. *Histopathology* 2020; **77**: 198-209 [PMID: 32364264 DOI: 10.1111/his.14134]

70 **Su H**, Yang M, Wan C, Yi LX, Tang F, Zhu HY, Yi F, Yang HC, Fogo AB, Nie X, Zhang C. Renal histopathological analysis of 26 postmortem findings of patients with COVID-19 in China. *Kidney Int* 2020; **98**: 219-227 [PMID: 32327202 DOI: 10.1016/j.kint.2020.04.003]

71 **Bhandari S**, Solanki R, Jindal A, Rankawat G, Pathak D, Bagarhatta M, Singh A. Demystifying COVID-19 lung pathology: A clinicopathological study of postmortem core needle biopsy. *Lung India* 2021; **38**: 343-349 [PMID: 34259173 DOI: 10.4103/lungindia.lungindia_919_20]

72 **Varga Z**, Flammer AJ, Steiger P, Haberecker M, Andermatt R, Zinkernagel AS, Mehra MR, Schuepbach RA, Ruschitzka F, Moch H. Endothelial cell infection and endotheliitis in COVID-19. *Lancet* 2020; **395**: 1417-1418 [PMID: 32325026 DOI: 10.1016/S0140-6736(20)30937-5]

73 **El Sissy C**, Saldman A, Zanetta G, Martins PV, Poulain C, Cauchois R, Kaplanski G, Venetz JP, Bobot M, Dobosziewicz H, Daniel L, Koubi M, Sadallah S, Rotman S, Mousson C, Pascual M, Frémeaux-Bacchi V, Fakhouri F. COVID-19 as a potential trigger of complement-mediated atypical HUS. *Blood* 2021; **138**: 1777-1782 [PMID: 34482396 DOI: 10.1182/blood.2021012752]

74 **Jamaly S**, Tsokos MG, Bhargava R, Brook OR, Hecht JL, Abdi R, Moulton VR, Satyam A, Tsokos GC. Complement activation and increased expression of Syk, mucin-1 and CaMK4 in kidneys of patients with COVID-19. *Clin Immunol* 2021; **229**: 108795 [PMID: 34252574 DOI: 10.1016/j.clim.2021.108795]

75 **Skendros P**, Mitsios A, Chrysanthopoulou A, Mastellos DC, Metallidis S, Rafailidis P, Ntinopoulou M, Sertaridou E, Tsironidou V, Tsigalou C, Tektonidou M, Konstantinidis T, Papagoras C, Mitroulis I, Germanidis G, Lambris JD, Ritis K. Complement and tissue factor-enriched neutrophil extracellular traps are key drivers in COVID-19 immunothrombosis. *J Clin Invest* 2020; **130**: 6151-6157 [PMID: 32759504 DOI: 10.1172/JCI141374]

76 **Diorio C**, McNerney KO, Lambert M, Paessler M, Anderson EM, Henrickson SE, Chase J, Liebling EJ, Burudpakdee C, Lee JH, Balamuth FB, Blatz AM, Chiotos K, Fitzgerald JC, Giglia TM, Gollomp K, Odom John AR, Jasen C, Leng T, Petrosa W, Vella LA, Witmer C, Sullivan KE, Laskin BL, Hensley SE, Bassiri H, Behrens EM, Teachey DT. Evidence of

thrombotic microangiopathy in children with SARS-CoV-2 across the spectrum of clinical presentations. *Blood Adv* 2020; **4**: 6051-6063 [PMID: 33290544 DOI: 10.1182/bloodadvances.2020003471]

77 **Cugno M**, Meroni PL, Gualtierotti R, Griffini S, Grovetti E, Torri A, Lonati P, Grossi C, Borghi MO, Novembrino C, Boscolo M, Uceda Renteria SC, Valenti L, Lamorte G, Manunta M, Prati D, Pesenti A, Blasi F, Costantino G, Gori A, Bandera A, Tedesco F, Peyvandi F. Complement activation and endothelial perturbation parallel COVID-19 severity and activity. *J Autoimmun* 2021; **116**: 102560 [PMID: 33139116 DOI: 10.1016/j.jaut.2020.102560]

78 **Frumholtz L**, Bouaziz JD, Battistella M, Hadjadj J, Chocron R, Bengoufa D, Le Buanec H, Barnabei L, Meynier S, Schwartz O, Grzelak L, Smith N, Charbit B, Duffy D, Yatim N, Calugareanu A, Philippe A, Guerin CL, Joly B, Siguret V, Jaume L, Bachelez H, Bagot M, Rieux-Laucat F, Maylin S, Legoff J, Delaugerre C, Gendron N, Smadja DM, Cassius C; Saint-Louis CORE (COvid REsearch). Type I interferon response and vascular alteration in chilblain-like lesions during the COVID-19 outbreak. *Br J Dermatol* 2021; **185**: 1176-1185 [PMID: 34611893 DOI: 10.1111/bjd.20707]

79 **Showers CR**, Nuovo GJ, Lakhanpal A, Siegel CH, Aizer J, Elreda L, Halevi A, Lai AR, Erkan D, Magro CM. A Covid-19 Patient with Complement-Mediated Coagulopathy and Severe Thrombosis. *Pathobiology* 2021; **88**: 28-36 [PMID: 33137805 DOI: 10.1159/000512503]

80 **Laurence J**, Mulvey JJ, Seshadri M, Racanelli A, Harp J, Schenck EJ, Zappetti D, Horn EM, Magro CM. Anti-complement C5 therapy with eculizumab in three cases of critical COVID-19. *Clin Immunol* 2020; **219**: 108555 [PMID: 32771488 DOI: 10.1016/j.clim.2020.108555]

81 **Gill SE**, Dos Santos CC, O'Gorman DB, Carter DE, Patterson EK, Slessarev M, Martin C, Daley M, Miller MR, Cepinskas G, Fraser DD; Lawson COVID19 Study Team. Transcriptional profiling of leukocytes in critically ill COVID19 patients: implications for interferon response and coagulation. *Intensive Care Med Exp* 2020; **8**: 75 [PMID: 33306162 DOI: 10.1186/s40635-020-00361-9]

82 **Barberis E**, Vanella VV, Falasca M, Caneapero V, Cappellano G, Raineri D, Ghirimoldi M, De Giorgis V, Puricelli C, Vaschetto R, Sainaghi PP, Bruno S, Sica A, Dianzani U, Rolla R, Chiocchetti A, Cantaluppi V, Baldanzi G, Marengo E, Manfredi M. Circulating Exosomes Are Strongly Involved in SARS-CoV-2 Infection. *Front Mol Biosci* 2021; **8**: 632290 [PMID: 33693030 DOI: 10.3389/fmolb.2021.632290]

83 **Freda CT**, Yin W, Ghebrehiwet B, Rubenstein DA. SARS-CoV-2 Structural Proteins Exposure Alter Thrombotic and Inflammatory Responses in Human Endothelial Cells. *Cell Mol Bioeng* 2021; 1-11 [PMID: 34484458 DOI: 10.1007/s12195-021-00696-7]

84 **Kaiser R**, Leunig A, Pekayvaz K, Popp O, Joppich M, Polewka V, Escaig R, Anjum A, Hoffknecht ML, Gold C, Brambs S, Engel A, Stockhausen S, Knottenberg V, Titova A, Haji M, Scherer C, Muenchhoff M, Hellmuth JC, Saar K, Schubert B, Hilgendorff A, Schulz C, Kääb S, Zimmer R, Hübner N, Massberg S, Mertins P, Nicolai L, Stark K. Self-sustaining IL-8 loops drive a prothrombotic neutrophil phenotype in severe COVID-19. *JCI Insight* 2021; **6** [PMID: 34403366 DOI: 10.1172/jci.insight.150862]

85 **Porto BN**, Stein RT. Neutrophil Extracellular Traps in Pulmonary Diseases: Too Much of a Good Thing? *Front Immunol* 2016; **7**: 311 [PMID: 27574522 DOI: 10.3389/fimmu.2016.00311]

86 **Vlaar APJ**, de Bruin S, Busch M, Timmermans SAMEG, van Zeggeren IE, Koning R, Ter Horst L, Bulle EB, van Baarle FEHP, van de Poll MCG, Kemper EM, van der Horst ICC, Schultz MJ, Horn J, Paulus F, Bos LD, Wiersinga WJ, Witzenrath M, Rueckinger S, Pilz K, Brouwer MC, Guo RF, Heunks L, van Paassen P, Riedemann NC, van de Beek D. Anti-C5a antibody IFX-1 (vilobelimab) treatment versus best supportive care for patients with severe COVID-19 (PANAMO): an exploratory, open-label, phase 2 randomised controlled trial. *Lancet Rheumatol* 2020; **2**: e764-e773 [PMID: 33015643 DOI: 10.1016/S2665-9913(20)30341-6]

87 **Kulasekararaj AG**, Lazana I, Large J, Posadas K, Eagleton H, Lord Villajin J, Zuckerman M, Gandhi S, Marsh JCW. Terminal complement inhibition dampens the inflammation during COVID-19. *Br J Haematol* 2020; **190**: e141-e143 [PMID: 32495372 DOI: 10.1111/bjh.16916]

88 **Diurno F**, Numis FG, Porta G, Cirillo F, Maddaluno S, Ragozzino A, De Negri P, Di Gennaro C, Pagano A, Allegorico E, Bressy L, Bosso G, Ferrara A, Serra C, Montisci A, D'Amico M, Schiano Lo Morello S, Di Costanzo G, Tucci AG, Marchetti P, Di Vincenzo U, Sorrentino I, Casciotta A, Fusco M, Buonerba C, Berretta M, Ceccarelli M, Nunnari G, Diessa Y, Cicala S, Facchini G. Eculizumab treatment in patients with COVID-19: preliminary results from real life ASL Napoli 2 Nord experience. *Eur Rev Med Pharmacol Sci* 2020; **24**: 4040-4047 [PMID: 32329881 DOI: 10.26355/eurrev_202004_20875]

89 **Zelek WM**, Cole J, Ponsford MJ, Harrison RA, Schroeder BE, Webb N, Jolles S, Fegan C, Morgan M, Wise MP, Morgan BP. Complement Inhibition with the C5 Blocker LFG316 in Severe COVID-19. *Am J Respir Crit Care Med* 2020; **202**: 1304-1308 [PMID: 32897730 DOI: 10.1164/rccm.202007-2778LE]

90 **Posch W**, Vosper J, Noureen A, Zaderer V, Witting C, Bertacchi G, Gstir R, Filipek PA, Bonn GK, Huber LA, Bellmann-Weiler R, Lass-Flörl C, Wilflingseder D. C5aR inhibition of nonimmune cells suppresses inflammation and maintains epithelial integrity in SARS-CoV-2-infected primary human airway epithelia. *J Allergy Clin Immunol* 2021; **147**: 2083-2097.e6 [PMID: 33852936 DOI: 10.1016/j.jaci.2021.03.038]

91 **Araten DJ**, Belmont HM, Schaefer-Cutillo J, Iyengar A, Mattoo A, Reddy R. Mild Clinical Course of COVID-19 in 3 Patients Receiving Therapeutic Monoclonal Antibodies Targeting C5 Complement for Hematologic Disorders. *Am J Case Rep* 2020; **21**: e927418 [PMID: 32917848 DOI: 10.12659/AJCR.927418]

92 **Iluta S**, Pasca S, Dima D, Mester G, Urian L, Bojan A, Zdrenghea M, Trifa A, Balacescu O, Tomuleasa C. Haematology patients infected with SARS-CoV-2, pretreated with eculizumab or siltuximab, develop oligosymptomatic disease. *Eur J Hosp Pharm* 2021 [PMID: 33541912 DOI: 10.1136/ejhpharm-2021-002694]

93 **Annane D**, Heming N, Grimaldi-Bensouda L, Frémeaux-Bacchi V, Vigan M, Roux AL, Marchal A, Michelon H, Rottman M, Moine P; Garches COVID 19 Collaborative Group. Eculizumab as an emergency treatment for adult patients with severe COVID-19 in the intensive care unit: A proof-of-concept study. *EClinicalMedicine* 2020; **28**: 100590 [PMID: 33173853 DOI: 10.1016/j.eclinm.2020.100590]

94 **Genthon A**, Chiarabini T, Baylac P, Valin N, Urbina T, Pacanowski J, Mekinian A, Brissot E, M 'Hammedi-Bouzina F, Lapusan S, Mohty M, Lacombe K, Ingiliz P. Severe COVID-19 infection in a patient with paroxysmal nocturnal

hemoglobinuria on eculizumab therapy. *Leuk Lymphoma* 2021; **62**: 1502-1505 [PMID: 33416421 DOI: 10.1080/10428194.2020.1869963]

95 **Giudice V**, Pagliano P, Vatrella A, Masullo A, Poto S, Polverino BM, Gammaldi R, Maglio A, Sellitto C, Vitale C, Serio B, Cuffa B, Borrelli A, Vecchione C, Filippelli A, Selleri C. Combination of Ruxolitinib and Eculizumab for Treatment of Severe SARS-CoV-2-Related Acute Respiratory Distress Syndrome: A Controlled Study. *Front Pharmacol* 2020; **11**: 857 [PMID: 32581810 DOI: 10.3389/fphar.2020.00857]

96 **Mastaglio S**, Ruggeri A, Risitano AM, Angelillo P, Yancopoulou D, Mastellos DC, Huber-Lang M, Piemontese S, Assanelli A, Garlanda C, Lambris JD, Ciceri F. The first case of COVID-19 treated with the complement C3 inhibitor AMY-101. *Clin Immunol* 2020; **215**: 108450 [PMID: 32360516 DOI: 10.1016/j.clim.2020.108450]

97 **Mastellos DC**, Pires da Silva BGP, Fonseca BAL, Fonseca NP, Auxiliadora-Martins M, Mastaglio S, Ruggeri A, Sironi M, Radermacher P, Chrysanthopoulou A, Skendros P, Ritis K, Manfra I, Iacobelli S, Huber-Lang M, Nilsson B, Yancopoulou D, Connolly ES, Garlanda C, Ciceri F, Risitano AM, Calado RT, Lambris JD. Complement C3 vs C5 inhibition in severe COVID-19: Early clinical findings reveal differential biological efficacy. *Clin Immunol* 2020; **220**: 108598 [PMID: 32961333 DOI: 10.1016/j.clim.2020.108598]

98 **Bouillet L**, Boccon-Gibod I, Gompel A, Floccard B, Martin L, Blanchard-Delaunay C, Launay D, Fain O. Hereditary angioedema with normal C1 inhibitor: clinical characteristics and treatment response with plasma-derived human C1 inhibitor concentrate (Berinert®) in a French cohort. *Eur J Dermatol* 2017; **27**: 155-159 [PMID: 28251901 DOI: 10.1684/ejd.2016.2948]

99 **Valerieva A**, Caccia S, Cicardi M. Recombinant human C1 esterase inhibitor (Conestat alfa) for prophylaxis to prevent attacks in adult and adolescent patients with hereditary angioedema. *Expert Rev Clin Immunol* 2018; **14**: 707-718 [PMID: 30021471 DOI: 10.1080/1744666X.2018.1503055]

100 **Weiler JM**, Edens RE, Linhardt RJ, Kapelanski DP. Heparin and modified heparin inhibit complement activation in vivo. *J Immunol* 1992; **148**: 3210-3215 [PMID: 1578145]

101 **Gozzo L**, Viale P, Longo L, Vitale DC, Drago F. The Potential Role of Heparin in Patients With COVID-19: Beyond the Anticoagulant Effect. A Review. *Front Pharmacol* 2020; **11**: 1307 [PMID: 32973526 DOI: 10.3389/fphar.2020.01307]

102 **Schoenfeld AK**, Lahrsen E, Alban S. Regulation of Complement and Contact System Activation *via* C1 Inhibitor Potentiation and Factor XIIa Activity Modulation by Sulfated Glycans - Structure-Activity Relationships. *PLoS One* 2016; **11**: e0165493 [PMID: 27783665 DOI: 10.1371/journal.pone.0165493]

103 **Urwyler P**, Moser S, Charitos P, Heijnen IAFM, Rudin M, Sommer G, Giannetti BM, Bassetti S, Sendi P, Trendelenburg M, Osthoff M. Treatment of COVID-19 With Conestat Alfa, a Regulator of the Complement, Contact Activation and Kallikrein-Kinin System. *Front Immunol* 2020; **11**: 2072 [PMID: 32922409 DOI: 10.3389/fimmu.2020.02072]

104 **Riedl MA**, Bygum A, Lumry W, Magerl M, Bernstein JA, Busse P, Craig T, Frank MM, Edelman J, Williams-Herman D, Feuersenger H, Rojavin M; Berinert Registry investigators. Safety and Usage of C1-Inhibitor in Hereditary Angioedema: Berinert Registry Data. *J Allergy Clin Immunol Pract* 2016; **4**: 963-971 [PMID: 27286778 DOI: 10.1016/j.jaip.2016.04.018]

105 **Davis B**, Bernstein JA. Conestat alfa for the treatment of angioedema attacks. *Ther Clin Risk Manag* 2011; **7**: 265-273 [PMID: 21753889 DOI: 10.2147/TCRM.S15544]

106 **Yuan X**, Gavriilaki E, Thanassi JA, Yang G, Baines AC, Podos SD, Huang Y, Huang M, Brodsky RA. Small-molecule factor D inhibitors selectively block the alternative pathway of complement in paroxysmal nocturnal hemoglobinuria and atypical hemolytic uremic syndrome. *Haematologica* 2017; **102**: 466-475 [PMID: 27810992 DOI: 10.3324/haematol.2016.153312]

107 **Rambaldi A**, Gritti G, Micò MC, Frigeni M, Borleri G, Salvi A, Landi F, Pavoni C, Sonzogni A, Gianatti A, Binda F, Fagiuoli S, Di Marco F, Lorini L, Remuzzi G, Whitaker S, Demopulos G. Endothelial injury and thrombotic microangiopathy in COVID-19: Treatment with the lectin-pathway inhibitor narsoplimab. *Immunobiology* 2020; **225**: 152001 [PMID: 32943233 DOI: 10.1016/j.imbio.2020.152001]

108 **Lafayette RA**, Rovin BH, Reich HN, Tumlin JA, Floege J, Barratt J. Safety, Tolerability and Efficacy of Narsoplimab, a Novel MASP-2 Inhibitor for the Treatment of IgA Nephropathy. *Kidney Int Rep* 2020; **5**: 2032-2041 [PMID: 33163724 DOI: 10.1016/j.ekir.2020.08.003]

109 **Rambaldi A**, Smith M, Whitaker S, Khaled, Samer. Narsoplimab (OMS721) for the treatment of adult hematopoietic stem cell transplant-associated thrombotic microangiopathy. *Eur Hematol Assoc Congr* 2020. Available from: https://Library.ehaweb.org/eha/2020/eha25th/295082/alessandro.rambaldi.narsoplimab.28oms72129.for.the.treatment.of.adult.html

110 **Kang S**, Yang M, He S, Wang Y, Chen X, Chen YQ, Hong Z, Liu J, Jiang G, Chen Q, Zhou Z, Huang Z, Huang X, He H, Zheng W, Liao HX, Xiao F, Shan H, Chen S. A SARS-CoV-2 antibody curbs viral nucleocapsid protein-induced complement hyperactivation. *Nat Commun* 2021; **12**: 2697 [PMID: 33976229 DOI: 10.1038/s41467-021-23036-9]

111 **Risitano AM**, Mastellos DC, Huber-Lang M, Yancopoulou D, Garlanda C, Ciceri F, Lambris JD. Complement as a target in COVID-19? *Nat Rev Immunol* 2020; **20**: 343-344 [PMID: 32327719 DOI: 10.1038/s41577-020-0320-7]

112 **Apellis Pharmaceuticals**, Inc. A Randomized, Double-Blinded, Vehicle-Controlled, Multicenter, Parallel-Group Study of APL-9 in Mild to Moderate Acute Respiratory Distress Syndrome Due to COVID-19. clinicaltrials.gov. Available from: https://clinicaltrials.gov/ct2/show/study/NCT04402060

113 **Dupont T**, Caillat-Zucman S, Fremeaux-Bacchi V, Morin F, Lengliné E, Darmon M, Peffault de Latour R, Zafrani L, Azoulay E, Dumas G. Identification of Distinct Immunophenotypes in Critically Ill Coronavirus Disease 2019 Patients. *Chest* 2021; **159**: 1884-1893 [PMID: 33316234 DOI: 10.1016/j.chest.2020.11.049]

114 **Mehlhop E**, Nelson S, Jost CA, Gorlatov S, Johnson S, Fremont DH, Diamond MS, Pierson TC. Complement protein C1q reduces the stoichiometric threshold for antibody-mediated neutralization of West Nile virus. *Cell Host Microbe* 2009; **6**: 381-391 [PMID: 19837377 DOI: 10.1016/j.chom.2009.09.003]

115 **Kurtovic L**, Beeson JG. Complement Factors in COVID-19 Therapeutics and Vaccines. *Trends Immunol* 2021; **42**: 94-103 [PMID: 33402318 DOI: 10.1016/j.it.2020.12.002]

116 **Seow J**, Graham C, Merrick B, Acors S, Pickering S, Steel KJA, Hemmings O, O'Byrne A, Kouphou N, Galao RP, Betancor G, Wilson HD, Signell AW, Winstone H, Kerridge C, Huettner I, Jimenez-Guardeño JM, Lista MJ, Temperton

N, Snell LB, Bisnauthsing K, Moore A, Green A, Martinez L, Stokes B, Honey J, Izquierdo-Barras A, Arbane G, Patel A, Tan MKI, O'Connell L, O'Hara G, MacMahon E, Douthwaite S, Nebbia G, Batra R, Martinez-Nunez R, Shankar-Hari M, Edgeworth JD, Neil SJD, Malim MH, Doores KJ. Longitudinal observation and decline of neutralizing antibody responses in the three months following SARS-CoV-2 infection in humans. *Nat Microbiol* 2020; **5**: 1598-1607 [PMID: 33106674 DOI: 10.1038/s41564-020-00813-8]

117 **Greinacher A**, Thiele T, Warkentin TE, Weisser K, Kyrle PA, Eichinger S. Thrombotic Thrombocytopenia after ChAdOx1 nCov-19 Vaccination. *N Engl J Med* 2021; **384**: 2092-2101 [PMID: 33835769 DOI: 10.1056/NEJMoa2104840]

World Journal of Experimental Medicine

Submit a Manuscript: https://www.f6publishing.com

World J Exp Med 2022 July 20; 12(4): 68-91

DOI: 10.5493/wjem.v12.i4.68

ISSN 2220-315x (online)

ORIGINAL ARTICLE

Randomized Controlled Trial

Comparative evaluation of effect of injectable platelet-rich fibrin with collagen membrane compared with collagen membrane alone for gingival recession coverage

Laxmikanta Patra, Subash Chandra Raj, Neelima Katti, Devapratim Mohanty, Shib Shankar Pradhan, Shaheda Tabassum, Asit Kumar Mishra, Kaushik Patnaik, Annuroopa Mahapatra

Specialty type: Dentistry, oral surgery and medicine

Provenance and peer review: Invited article; Externally peer reviewed.

Peer-review model: Single blind

Peer-review report's scientific quality classification

Grade A (Excellent): 0
Grade B (Very good): B
Grade C (Good): 0
Grade D (Fair): 0
Grade E (Poor): 0

P-Reviewer: Bennardo F, Italy

Received: December 18, 2021
Peer-review started: December 18, 2021
First decision: April 13, 2022
Revised: April 26, 2022
Accepted: June 23, 2022
Article in press: June 23, 2022
Published online: July 20, 2022

Laxmikanta Patra, Subash Chandra Raj, Neelima Katti, Devapratim Mohanty, Shib Shankar Pradhan, Shaheda Tabassum, Asit Kumar Mishra, Kaushik Patnaik, Annuroopa Mahapatra, Department of Periodontics, SCB Dental College and Hospital, Odisha 753007, India

Corresponding author: Subash Chandra Raj, MDS, Associate Professor, Department of Periodontics, SCB Dental College and Hospital, Mangalabag Road, Cuttack, Odisha 753007, India. drsubash007@gmail.com

Abstract

BACKGROUND

Collagen membrane and platelet-rich fibrin (PRF) have emerged as vital biomaterials in the field of periodontal regeneration. Minimally invasive techniques are being preferred by most periodontists, as it is patient compliant with fewer post-surgical complications as compared to conventional surgical techniques. Thus, in this study we have evaluated the effect of injectable PRF (i-PRF) with collagen membrane compared with collagen membrane alone using vestibular incision subperiosteal tunnel access (VISTA) technique for gingival recession coverage.

AIM

To compare the efficacy of VISTA using collagen membrane with collagen membrane soaked in injectable PRF for gingival recession coverage.

METHODS

A split mouth randomized controlled clinical trial was designed;13 subjects having at least 2 teeth indicated for recession coverage were enrolled in this study. The sites were randomly assigned to control group (VISTA using collagen membrane alone) and the test group (VISTA using collagen membrane with i-PRF). The clinical parameters assessed were pocket depth, recession depth (RD), recession width (RW), relative attachment level, keratinised tissue width (KTW), keratinised tissue thickness (KTT), and percentage root coverage.

RESULTS

RD showed a statistically significant difference between the test group at 3 mo (0.5

± 0.513) and 6 mo (0.9 ± 0.641) and the control group at 3 mo (0.95 ± 0.51) and 6 mo (1.5 ± 0.571), with *P* values of 0.008 and 0.04, respectively. RW also showed a statistically significant difference between the test group at 3 mo (1 ± 1.026) and 6 mo (1.65 ± 1.04) and the control group at 3 mo (1.85 ± 0.875) and 6 mo (2.25 ± 0.759), with *P* values of 0.008 and 0.001, respectively. Results for KTW showed statistically significant results between the test group at 1 mo (2.85 ± 0.489), 3 mo (3.5 ± 0.513), and 6 mo (3.4 ± 0.598) and the control group at 1 mo (2.45 ± 0.605), 3 mo (2.9 ± 0.447), and 6 mo (2.75 ± 0.444), with *P* values of 0.04, 0.004, and 0.003, respectively. Results for KTT also showed statistically significant results between test group at 1 mo (2.69 ± 0.233), 3 mo (2.53 ± 0.212), and 6 mo (2.46 ± 0.252) and the control group at 1 mo (2.12 ± 0.193), 3 mo (2.02 ± 0.18), and 6 mo (1.91 ± 0.166), with *P* values of 0.001, 0.001, and 0.001, respectively. The test group showed 91.6%, 81.6%, and 67% root coverage at 1 mo, 3 mo, and 6 mo, while the control group showed 82.3%, 66.4%, and 53.95% of root coverage at 1 mo, 3 mo, and 6 mo, respectively.

CONCLUSION

The use of minimally invasive VISTA technique along with collagen membrane and injectable form of platelet-rich fibrin can be successfully used as a treatment method for multiple or isolated gingival recessions of Miller's class-I and class-II defects.

Key Words: Vestibular incision subperiosteal tunnel access; Injectable platelet-rich fibrin; Collagen membrane; Gingival recessions; Treatment

Core Tip: The use of minimally invasive vestibular incision subperiosteal tunnel access technique, along with collagen membrane acting as scaffold and chemoattractant with added benefit of injectable form of platelet-rich fibrin has the capacity of releasing more growth factors and regenerative cells responsible for tissue regeneration, can be successfully used as a treatment method for multiple or isolated gingival recessions of Miller's class-I and class-II defects.

Citation: Patra L, Raj SC, Katti N, Mohanty D, Pradhan SS, Tabassum S, Mishra AK, Patnaik K, Mahapatra A. Comparative evaluation of effect of injectable platelet-rich fibrin with collagen membrane compared with collagen membrane alone for gingival recession coverage. *World J Exp Med* 2022; 12(4): 68-91
URL: https://www.wjgnet.com/2220-315x/full/v12/i4/68.htm
DOI: https://dx.doi.org/10.5493/wjem.v12.i4.68

INTRODUCTION

Gingival recession is a common feature affecting large populations leading to functional and aesthetic problems. While inflammation is the main etiologic factor for gingival recession, other anatomical factors, like thin biotype, abnormal tooth position (positioned too far buccally or lingually, direct trauma associated with malocclusion, aberrant frenal attachment, class-II division 2 malocclusion), and iatrogenic factors, like mechanical trauma (impaction of foreign bodies, faulty tooth brushing, poorly designed partial dentures) can also cause gingival recession. Subgingival restoration margins, the presence of calculus, periodontal disease, and smoking also plays role in the etiology of gingival recession[1-3].

Gingival recession is being treated using various therapeutic approaches with varying degrees of success depending on the etiology and treatment approach. Various periodontal surgical techniques for root coverage, like free gingival graft (FGG), subepithelial connective tissue graft (SCTG), semilunar flap, coronally advanced flap (CAF), and guided tissue regeneration (GTR), are available. Among them, CAF with connective tissue graft (CTG) is considered the gold standard for soft tissue augmentation and periodontal root coverage. It has some disadvantages, including harvesting from a donor site, limited tissue availability, and increased potential for post-harvesting morbidity[4].

With the introduction of various minimally invasive tunnelling techniques for gingival augmentation, similar results could be obtained. It tries to preserve the interdental papillae, unhampered blood supply, and faster wound healing. However, these procedures are quite technique sensitive and may cause tissue trauma to the sulcular epithelium leading to unfavorable healing outcomes[5].

To avoid these complications, a new minimally invasive approach for treating multiple gingival recession defects within the maxillary and mandibular aesthetic zone was introduced by Zadeh[4] called the vestibular incision subperiosteal tunnel access (VISTA) technique. Complete root coverage was

observed for all VISTA treated sites along with a 1-2 mm gain in keratinised gingiva at the end of 12th mo follow-up period. These improvements were sustained at the 20th mo observation period[4]. Mansouri *et al*[6] compared the VISTA technique with the gold standard coronally advanced flap (CAF) technique using CTG for the treatment of gingival recession defects, which showed higher frequency of root coverage with the VISTA technique as compared to CAF. Mohamed *et al*[7] compared the efficacy of the VISTA technique with the tunnel technique (TUN) using acellular dermal matrix (ADM) allograft for gingival recession coverage. The 6-mo follow up results showed a statistically significant difference in favor of the VISTA + ADM technique than the TUN + ADM technique. This minimally invasive procedure promises adequate blood supply to the surgical site as it requires a small opening leading to the undermining of the periosteum, completely free from the area of root coverage, which further enhances the coronal positioning of the flap passively onto the exposed root surface[3].

Along with various techniques for root coverage procedure, several grafts, such as CTG, ADM allograft, Amniotic membrane, and bioactive glass, can be advocated for root coverage[3]. Adjunctive agents, like recombinant human growth factor, platelet rich plasma (PRP), and platelet-rich fibrin (PRF) have been used to accelerate healing and enhance clinical outcomes[3,8].

Collagen membrane is one of the materials used for gingival recession coverage, It is semipermeable, which allows nutrient passage and gas exchange and supports cell proliferation *via* its lattice-like structure and cell binding ability. It increases tissue volume as it is naturally absorbed and is replaced by host tissue. The chemotactic function encourages host cell migration and attachment, thus facilitating primary wound closure and reducing the likelihood of membrane exposure or potential wound/membrane contamination[9].

Another agent that is commonly used for recession coverage is PRF, which is a leukocyte and platelet-rich fibrin biomaterial with a specific composition and 3D architecture that plays an important role in the release of growth factors, immune regulation, anti-infectious activities, and matrix remodeling during wound healing, and further serves as a scaffold for tissue regeneration by acting as a barrier membrane in guided bone regeneration (GBR) and guided tissue regeneration (GTR) procedures[10-14]. PRF has been utilized for the treatment of extraction sockets, gingival recessions, palatal wound closure, regeneration of periodontal defects, and hyperplastic gingival tissues[15].

Initially, PRF formulations were lacking a liquid concentrate of proteins, as standardized PRF had the majority of its growth factor encapsulated within its fibrin matrix. Recent advances in the field aim at developing a liquid formulation of PRF with no anticoagulants or fibrin matrix to allow the development of an injectable formulation of PRF, termed injectable PRF (i-PRF), which is a platelet concentrate in a liquid formulation that can be either utilized alone or combined easily with various biomaterials. It has a higher presence of regenerative cells with higher concentrations of growth factors and higher fibroblast migration, and has a higher expression of platelet-derived growth factor (PDGF), transforming growth factor (TGF-β), and type-1 collagen when compared to other formulations of PRF [16,17].

The purpose of the study was to compare the efficacy of the VISTA technique incorporating collagen membrane alone with the VISTA technique with collagen membrane soaked in injectable platelet-rich fibrin for gingival recession coverage.

MATERIALS AND METHODS

The study was recommended by the Institutional Ethics Committee, under IEC/SCBDCH/049/20189 dated September 17, 2019 before its commencement and was conducted in accordance with the declaration of Helsinki of 1975 as revised in 2000. This was an interventional, parallel design, double blinded, randomized controlled trial performed from March 2020 to March 2021 in our department. A written informed consent was obtained from all participants after they received a written and oral explanation of study objectives, risks, and benefits. The study was prospectively registered with clinical trials registry (CTRI/2020/06/026141).

Patient selection

Sample size was calculated using G power 3.1.9.2 software (SPSS software India by Norman H Nie in 2015 G Power 3.1.9.2) considering 80% power, a 95%CI level with an effect size of 0.55 and a mean probing depth of 2.27mm before the treatment and 2.08mm after the treatment with a standard deviation of 0.34 mm respectively.

Inclusion criteria: (1) Both males and females of age ≥ 18 years with dentinal hypersensitivity or impaired aesthetics or difficulty in oral hygiene maintenance associated with gingival recession; (2) Subjects having Miller class I or II bilateral buccal gingival recession defects measuring ≥ 2 mm on the anterior teeth or premolars, on either arch; (3) Subjects who are not on any medication known to interfere with periodontal tissue health or healing within 6 mo of the study; and (4) Subjects having identifiable cementoenamel junction (CEJ) at recession sites.

Exclusion criteria: (1) History of systemic diseases (*i.e.* diabetes, autoimmune dysfunction, prolonged cortisone therapy, or chemotherapy) that would contraindicate periodontal surgical treatment; (2)

Patients with deleterious habits like the use of tobacco chewing or smoking; (3) History of previous periodontal surgical treatment of the involved sites; (4) Presence of malocclusion and pathologic movement of teeth in involved sites; and (5) Presence of active carious lesions, restorations, or crowns at the CEJ, as well as non-vital teeth with radicular grooves and irregularities.

Randomisation and allocation

A simple random sampling technique by coin toss was done by an author (SCR) unaware of the clinical parameters, to decide which side/arch to act as test site and which as to control site of each patient. In sites included in the test group, recession sites were placed with collagen membrane soaked with injectable platelet-rich fibrin and in the control site only collagen membrane was placed.

Preoperative protocol

After enrollment, all the participants underwent an initial non-surgical therapy including full mouth supra and subgingival scaling and root planning using ultrasonic scalers and hand instruments to ensure a healthy periodontium before the onset of surgical phase. Each of them was then given a standardized set of oral hygiene instructions both verbally and in a written format. Alginate impressions were taken 4 wk after signal recognition particle and study casts were poured. An acrylic template was fabricated on the study cast extending one tooth mesial and distal to the tooth indicated for extraction. This template was used as reference for the vertical measurements during the course of the study.

Clinical parameters

Clinical parameters were recorded at baseline (immediately before surgery) (Figure 1A and Figure 2A), as well as at 1 mo, 3 mo, and 6 mo follow-up appointments for control and test site groups. The clinical parameters recorded were as follows:

Plaque index (PI) as outlined by Silness P and Loe H (1964).

Gingival index (GI) as outlined by Loe H and Silness P (1963).

Probing depth (PD) measured with a UNC-15 periodontal probe as the distance from the gingival margin to the bottom of the pocket.

Recession depth (RD) was measured as the distance from the cementoenamel junction (CEJ) to the gingival margin at the mid-buccal surface using the UNC-15 probe.

Recession width (RW) was measured with a UNC-15 periodontal probe oriented horizontally and located at the most apical convexity of the CEJ, and horizontal distance between the mesial and distal gingival margin.

Relative attachment level (RAL) was measured mid-buccally with the reference point located at the apical end of the groove in the stent to the bottom of the periodontal pocket.

Keratinized tissue width (KTW) was measured from the most coronal extension of gingival margin to the mucogingival line.

Thickness of keratinized tissue (KTT) was measured by using an endodontic K-file (number-20, color code – yellow) with a silicon stop, perpendicular to the tissue surface and 2 mm apical to the gingival margin. After reaching the hard surface, the silicon stop was slid and placed in contact with the soft tissue. After removing the file, the distance between the tip of the file and the silicon stop was measured with a digital caliper accurate to the nearest 0.1 mm.

Percentage of root coverage was calculated according to the formula: % Root coverage = (Preoperative recession depth-Postoperative recession depth)/(Preoperative recession depth) × 100%.

Surgical protocol

After extraoral scrubbing with 5% povidone-iodine solution, the patient was asked to rinse with 10 mL of 0.2% chlorhexidine digluconate solution for 1 min. Root debridement was done with an ultrasonic instrument followed by odontoplasty, carried out where necessary using a rotary finishing bur. The surgical site was anesthetized by local infiltration (2% lidocaine HCL with adrenaline 1:100000). The roots are then conditioned for 2 min with 24% buffered ethylenediaminetetraacetic acid gel to eliminate the smear layer.

For the test site, the vestibular incision subperiosteal tunnel access (VISTA) approach began with a vestibular access incision at an optimal position to gain access to the recession defects. The location of the access incision depends on the sites being treated, *e.g.*, in cases where both premolars are indicated for recession coverage, the vertical access incision was given in between both the premolars. The incision was made through the periosteum using a No. 15 surgical blade (Bard-Parker) exposing the facial osseous plate (Figure 1B). A special set of patented periosteal elevators (VISTA 1-4) was used to elevate the periosteum and create the subperiosteal tunnel. The attached gingiva adjacent to the incision was elevated using VISTA 1, and the areas that are distant from the incision are elevated with VISTA 2, and interproximal areas were elevated with VISTA 3 and 4 instruments. With a VISTA 2 elevator, the tunnel was extended to at least one tooth beyond the teeth requiring root coverage, also beyond the mucogingival junction, and into the gingival sulcus of the teeth in the involved area, to aid in the mobilization of the mucoperiosteal flap (Figure 1C and D).

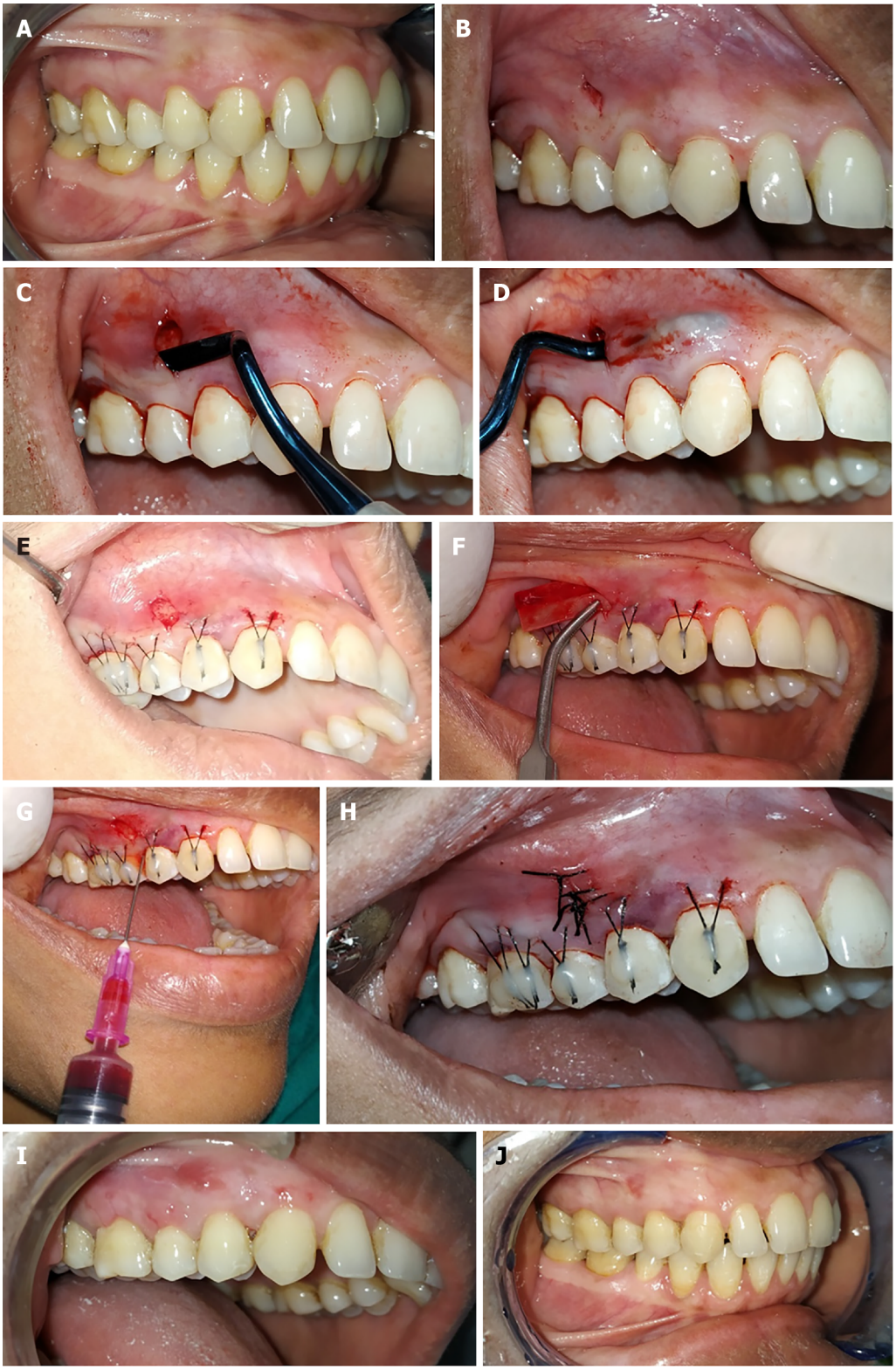

DOI: 10.5493/wjem.v12.i4.68

Figure 1 Vestibular incision subperiosteal tunnel access technique using collagen membrane along with injectable platelet-rich fibrin for the test sites. A: Preoperative photograph; B: Vertical access incision; C: Subperiosteal tunnel preparation on the distal side; D: Subperiosteal tunnel preparation on the mesial side; E: Coronally anchored suturing; F: Injectable platelet-rich fibrin (i-PRF) soaked collagen membrane placement into the tunnel; G: Injecting i-PRF into mesial, distal periodontal ligament and facial surface of gingiva; H: Final suturing; I: 1 mo follow-up; J: 6 mo follow-up.

The mucogingival complex was coronally positioned using an anchored horizontal mattress suture. An anchored horizontal mattress suture was placed at a distance of 2-3 mm from gingival margin using 5-0 black braided suture with 3/8 reverse cutting needle. These anchored sutures were coronally positioned. The knot of the anchored sutures was moved on the facial enamel surfaces of the involved teeth to check the final position of the coronally advanced mucogingival complex. After that, the facial

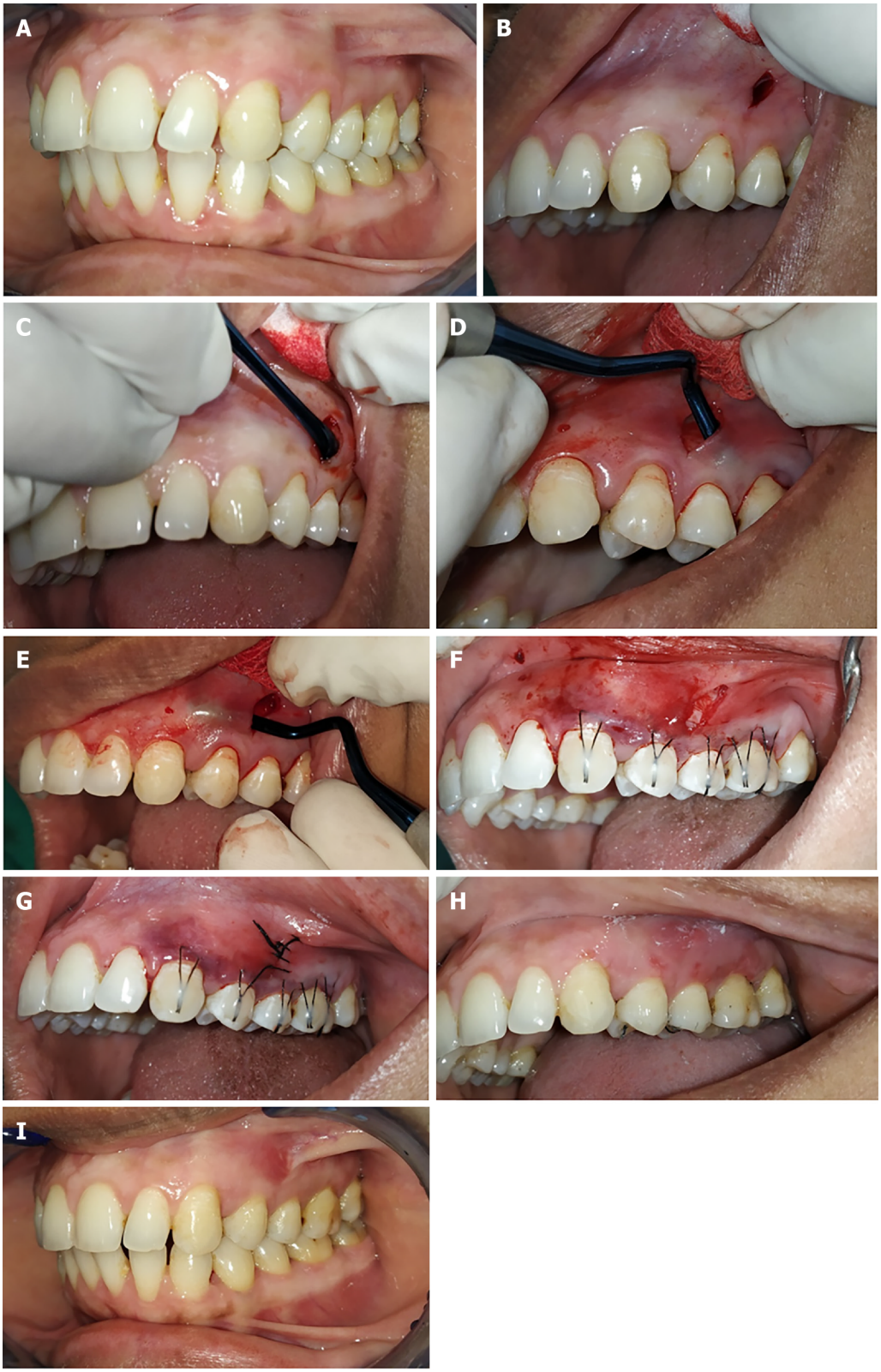

DOI: 10.5493/wjem.v12.i4.68

Figure 2 Vestibular incision subperiosteal tunnel access technique using collagen membrane alone for the control sites. A: Preoperative photograph; B: Vertical access incision (control site); C: Subperiosteal tunnel preparation on the distal side; D: Subperiosteal tunnel preparation on the distal side; E: Subperiosteal tunnel preparation on the mesial side; F: Collagen membrane placement into the tunnel; G: Final suturing; H: 1 mo follow-up; I: 6 mo follow-up.

enamel surfaces of each tooth were briefly etched for 15 s, irrigated for 15 s, and dried with air. Thereafter, a bonding agent was applied over the prepared enamel surface and light cured. Then knots of anchored sutures were secured to the prepared facial aspect of each tooth by placing a small amount of flowable composite resin over the knot and was light cured (Figure 1E). This procedure effectively prevents apical relapse of the gingival margin during the initial stages of healing.

For the i-PRF preparation, first a tourniquet was tied around the arm of the patient, the skin over the antecubital vein was disinfected with Surgical spirit. Two tubes of 10 mL whole blood were collected by venipuncture of the antecubital vein. The collected blood was centrifuged at 700 rpm for 3 min (60 × g) (according to Miron RJ) at room temperature without any additives in restriction enzyme-mediated integration laboratory centrifuge machine. The i-PRF formed at the top layer, which was immediately collected into a 2 mL syringe with a 25-gauge needle. Then, commercially available collagen membrane (HEALIGUIDE Bio resorbable membrane, Advanced Biotech Products, INDIA) was trimmed according to the size of recession in the experimental site, and the trimmed collagen membrane was soaked with i-PRF for 10 min in a steel bowl and inserted into the experimental site with the help of tissue forceps (Figure 1F). Along with this, i-PRF was also injected at the mesial and distal aspects into the periodontal ligament and the facial aspect of the gingiva (Figure 1G). Finally, the vertical access incision was approximated and sutured with 5-0 black braided silk sutures, achieving primary wound closure (Figure 1H).

For the control site, a similar surgical technique was used to prepare the tunnel on the control site (Figure 2B-E). After that, collagen membrane was trimmed according to the size of the recession at the control site and soaked with normal saline for 10 min before being inserted into the tunnel. Similar to the test site, 5-0 black braided silk sutures was used to close the vertical access incision for achieving primary closure (Figure 2F and G).

Post-operative care

All the patients were prescribed antibiotics and analgesics. Post-operative instructions were given to all patients and kept on a strict oral hygiene maintenance program. The vertical incision suture was removed after 1 wk and anchored sutures were removed after 3 wk post-surgery. The residual composite resin was removed using 16-flute tungsten carbide burs.

The follow-up was done every month for all the patients. During follow-up, oral prophylaxis was done and oral hygiene instructions were reinstituted. The measurements of clinical parameters were taken at 1, 3, and 6 mo postoperatively (Figure 1I and J, Figure 2H and I).

Statistical analysis

The data was analyzed using SPSS Ver 22 for windows, (IBM Corp, Armonik, United States). Descriptive statistics were expressed as a mean with standard deviations and proportions. Normally distributed data were analyzed using paired *t*-test for intragroup comparison and unpaired *t*-test for intergroup comparison. Skewed data were analyzed using the Wilcoxon signed rank test for intragroup and Mann-Whitney *U* test for intergroup comparison. The level of significance was set at $P < 0.05$.

RESULTS

The study consists of 13 subjects (7 males, 6 females) with the mean age of 36.7 ± 12.44 years (Table 1). All recession sites were divided into two groups: Group-I: Test sites (20 sites in which i-PRF with collagen membrane was used for recession coverage) and Group-II: Control sites (20 sites in which collagen membrane alone was used for recession coverage) (see flow diagram in Figure 3). Sample size was calculated using G power 3.1.9.2 software (SPSS software India by Norman H Nie in 2015 G Power 3.1.9.2).

Mean plaque index scores of the test group were 0.625 ± 0.151, 0.865 ± 0.134, 0.6 ± 0.133, and 0.54 ± 0.127 and of the control group were 0.625 ± 0.154, 0.835 ± 0.172, 0.545 ± 0.139, and 0.56 ± 0.134 at baseline, post-operative 1 mo, 3 mo, and 6 mo, respectively. The plaque scores are statistically not significant at different time intervals in the intergroup comparison (Table 2, Figure 4A). However, there was a statistically significant difference between mean scores in the intragroup comparison between each time interval for individual groups ($P < 0.01$). No statistically significant difference found between baseline and postoperative 3 mo for the test group ($P = 0.204$) and between postoperative 3 mo and 6 mo for control group ($P = 0.379$) (Table 3).

Mean gingival index scores of the test group were 0.625 ± 0.164, 0.89 ± 0.141, 0.545 ± 0.119, and 0.51 ± 0.149 and of the control group were 0.625 ± 0.65, 0.89 ± 0.18, 0.575 ± 0.155, and 0.51 ± 0.137 at baseline, post-operative 1 mo, 3 mo, and 6 mo, respectively. Intergroup comparison of gingival index scores revealed no statistically significant difference between mean scores at different time intervals (Table 4 and Figure 4B). However, there was a statistically significant increase in the gingival index scores between baseline and postoperative 1 mo for both groups ($P < 0.01$). There was a decrease in gingival index scores at subsequent time intervals for both the groups except between postoperative 3 mo and 6 mo ($P = 0.137$) (Table 5).

Mean probing depth scores of the test group were 1.75 ± 0.444 mm, 2.65 ± 0.489 mm, 2.05 ± 0.489 mm, and 1.75 ± 0.444 mm and of the control group were 2.05 ± 0.6 mm, 2.8 ± 0.83 mm, 2.1 ± 0.3 mm, and 1.95 ± 0.223 mm at baseline, postoperative 1 mo, 3 mo, and 6 mo, respectively. In the intergroup comparison between the test group and control group, there was no statistically significant difference between mean scores at the different time interval between two groups (Table 6 and Figure 4C). However, there was a

Table 1 Demographic characteristics and mean values of clinical parameters

Demographic characteristics		Test, mean ± SD	Control, mean ± SD
Sex			
Male	7		
Female	6		
Age	36.7 ± 12.44		
PI		0.625 ± 0.151	0.625 ± 0.154
GI		0.625 ± 0.164	0.625 ± 0.65
PD		1.75 ± 0.444	2.05 ± 0.6
RD		2.7 ± 0.86	2.9 ± 0.71
RW		3.5 ± 0.6	3.7 ± 0.73
RAL		7.3 ± 0.8	7.05 ± 0.82
KTW		1.6 ± 0.5	1.35 ± 0.48
KTT		1.64 ± 0.237	1.61 ± 0.201

GI: Gingival index; KTT: Keratinised tissue thickness; KTW: Keratinised tissue width; PD: Pocket depth; PI: Plaque index; RAL: Relative attachment level; RD: Recession depth; RW: Recession width.

Table 2 Intergroup comparison of mean plaque scores between injectable platelet-rich fibrin + collagen membrane and collagen membrane at different time intervals using unpaired *t* test

Time (mo)	Group	*n*	mean ± SD		*P* value
0	i-PRF + CM	20	0.625	0.15174	1.000
	CM	20	0.625	0.15174	NS
1	i-PRF + CM	20	0.865	0.13485	0.544
	CM	20	0.835	0.17252	NS
3	i-PRF + CM	20	0.6	0.13377	0.211
	CM	20	0.545	0.13945	NS
6	i-PRF + CM	20	0.54	0.12732	0.810
	CM	20	0.53	0.13416	NS

Level of significance at $P < 0.05$. CM: Collagen membrane; i-PRF: Injectable platelet-rich fibrin; NS: Not significant using unpaired *t* test.

significant increase in probing depth between baseline and 1 mo and subsequent decrease in probing depth at postoperative 1 mo, 3 mo, and 6 mo, respectively for test group. Similarly, in the control group, there was an increase in probing depth between baseline and 1 mo. Although there was a decrease in probing depth between postoperative 1 mo and 3 mo which was not statistically significant, but there was a significant decrease between postoperative 3 mo and 6 mo. There was no significant difference between baseline and postoperative 6 mo, and postoperative 1 mo and 6 mo respectively (Table 7).

Mean recession depth scores of the test group were 2.7 ± 0.86 mm, 0.25 ± 0.4 mm, 0.5 ± 0.5 mm, and 0.9 ± 0.64 mm and of the control group were 2.9 ± 0.71 mm, 0.5 ± 0.51 mm, 0.95 ± 0.51 mm, and 1.3 ± 0.57 mm at baseline, 1 mo, 3 mo, and 6 mo, respectively. In the intergroup analysis, there was no statistically significant difference between mean scores at baseline and 1 mo; however, there was a statistically significant difference in mean recession depth at 3 mo ($P < 0.01$) and 6 mo ($P < 0.05$) between both the test and control groups (Table 8 and Figure 4D). Within the group analysis, there was a statistically significant decrease in mean recession depth in both the groups between baseline and 1 mo ($P = 0.001$); 1 mo and 3 mo ($P = 0.021$; $P = 0.001$), and 3 mo and 6 mo ($P = 0.002$; $P = 0.005$), respectively (Table 9).

Mean recession width scores of the test group were 3.5 ± 0.6 mm, 0.5 ± 0.8 mm, 1 ± 1.02 mm, and 1.65 ± 1.03 mm and for the control group were 3.7 ± 0.73 mm, 1 ± 1.02 mm, 1.85 ± 0.85 mm, and 2.55 ± 0.75 mm at baseline, 1 mo, 3 mo and 6 mo, respectively. In the intergroup analysis, there was a statistically significant difference between the two groups at 3 mo ($P < 0.01$) and 6 mo ($P < 0.01$), respectively. There

Table 3 Intragroup comparison of mean plaque scores obtained by using injectable platelet-rich fibrin + collagen membrane and collagen membrane at different time intervals

i-PRF + CM in mo	mean ± SD	*P* value	CM in mo	mean ± SD	*P* value
0	0.625 ± 0.151	0.001[a]	0	0.625 ± 0.154	0.001[a]
1	0.865 ± 0.134		1	0.835 ± 0.172	
0	0.625 ± 0.151	0.204	0	0.625 ± 0.154	0.001[a]
3	0.6 ± 0.133		3	0.545 ± 0.139	
0	0.625 ± 0.151	0.001[a]	0	0.625 ± 0.154	0.001[a]
6	0.54 ± 0.127		6	0.53 ± 0.134	
1	0.865 ± 0.134	0.001[a]	1	0.835 ± 0.172	0.001[a]
3	0.6 ± 0.133		3	0.545 ± 0.139	
1	0.865 ± 0.134	0.001[a]	1	0.835 ± 0.172	0.001[a]
6	0.54 ± 0.127		6	0.56 ± 0.134	
3	0.6 ± 0.133	0.004[a]	3	0.545 ± 0.139	0.379
6	0.54 ± 0.127		6	0.56 ± 0.134	

[a]$P < 0.01$ statistically significant using paired *t* test.
Level of significance at $P < 0.05$. CM: Collagen membrane; i-PRF: Injectable platelet-rich fibrin.

Table 4 Intergroup comparison of mean gingival index scores between injectable platelet-rich fibrin + collagen membrane and collagen membrane at different time intervals using unpaired *t* test

mo	Group	*n*	mean ± SD	*P* value
0	i-PRF + CM	20	0.625 ± 0.16504	1.0
	CM	20	0.625 ± 0.16504	NS
1	i-PRF + CM	20	0.89 ± 0.14105	1.0
	CM	20	0.89 ± 0.18035	NS
3	i-PRF + CM	20	0.545 ± 0.1191	0.497
	CM	20	0.575 ± 0.15517	NS
6	i-PRF + CM	20	0.515 ± 0.14965	0.913
	CM	20	0.51 ± 0.13727	NS

Level of significance at $P < 0.05$. CM: Collagen membrane; i-PRF: Injectable platelet-rich fibrin; *n*: Number of frequency; NS: Not significant.

was no statistically significant difference at baseline and 1 mo (Table 10 and Figure 4E). In intragroup analysis, there was a statistically significant decrease in the recession width between baseline and 1 mo ($P = 0.001$), and an increase in the width of recession between 1 mo and 3 mo ($P = 0.025$; $P = 0.004$) in both groups, respectively. Similarly, there was an increase in the recession width between 3 mo and 6 mo ($P = 0.009$; $P = 0.001$) (Table 11).

Mean relative attachment scores for the test group were 7.3 ± 0.8 mm, 5.6 ± 1.3 mm, 5.25 ± 1.29 mm, and 5.55 ± 1.09 mm and for the control group were 7.05 ± 0.82 mm, 5.4 ± 0.94 mm, 5.05 ± 0.94 mm, and 5.45 ± 0.82 mm at baseline, 1 mo, 3 mo, and 6 mo, respectively. In intergroup analysis, there was a statistically significant difference between the two groups at 3 mo ($P < 0.01$) and 6 mo ($P < 0.01$), respectively (Table 12 and Figure 4F). There was no statistically significant difference at baseline and 1 mo. There was a statistically significant decrease in the attachment level in both the groups between baseline and 1 mo ($P = 0.001$). There was a further decrease in the test group between 1 mo and 3 mo ($P = 0.021$) and between 3 mo and 6 mo for the control group ($P = 0.021$) (Table 13).

The mean width of keratinized tissue scores for the test group were 1.6 ± 0.5 mm, 2.85 ± 0.48 mm, 3.5 ± 0.51 mm, and 3.4 ± 0.59 mm and for the control group were 1.35 ± 0.48 mm, 2.45 ± 0.6 mm, 2.9 ± 0.44 mm, and 2.75 ± 0.44 mm at baseline, 1 mo, 3 mo, and 6 mo, respectively. Intergroup comparison revealed statistically insignificant difference between the two groups at baseline, but there was a statist-

Table 5 Intragroup comparison of mean gingival index scores obtained by using injectable platelet-rich fibrin + collagen membrane and collagen membrane at different time intervals using paired *t* test

i-PRF + CM in mo	mean ± SD	*P* value	CM in mo	mean ± SD	*P* value
0	0.625 ± 0.164	0.001[a]	0	0.625 ± 0.165	0.001[a]
1	0.89 ± 0.141		1	0.89 ± 0.18	
0	0.625 ± 0.164	0.001[a]	0	0.625 ± 0.165	0.001[a]
3	0.545 ± 0.119		3	0.575 ± 0.155	
0	0.625 ± 0.164	0.001[a]	0	0.625 ± 0.165	0.001[a]
6	0.51 ± 0.149		6	0.51 ± 0.137	
1	0.89 ± 0.141	0.001[a]	1	0.89 ± 0.18	0.001[a]
3	0.545 ± 0.119		3	0.575 ± 0.155	
1	0.89 ± 0.141	0.001[a]	1	0.89 ± 0.18	0.001[a]
6	0.51 ± 0.149		6	0.51 ± 0.137	
3	0.545 ± 0.119	0.137	3	0.545 ± 0.155	0.137
6	0.51 ± 0.149		6	0.51 ± 0.137	

[a]*P* < 0.01 statistically significant.

Level of significance at *P* < 0.05. CM: Collagen membrane; i-PRF: Injectable platelet-rich fibrin.

Table 6 Intergroup comparison of mean pocket depth scores between injectable platelet-rich fibrin + collagen membrane and collagen membrane at different time intervals using unpaired *t* test

Time (mo)	Group	*n*	mean ± SD	*P* value
0	i-PRF + CM	20	1.75 ± 0.44426	0.082
	CM	20	2.05 ± 0.60481	NS
1	i-PRF + CM	20	2.65 ± 0.48936	0.492
	CM	20	2.8 ± 0.83351	NS
3	i-PRF + CM	20	2.05 ± 0.22361	0.560
	CM	20	2.1 ± 0.30779	NS
6	i-PRF + CM	20	1.75 ± 0.44426	0.080
	CM	20	1.95 ± 0.22361	NS

Level of significance at *P* < 0.05. CM: Collagen membrane; i-PRF: Injectable platelet-rich fibrin; *n*: Number of frequency; NS: Not significant.

ically significant difference at 1 mo, 3 mo, and 6 mo, respectively (Table 14 and Figure 4G). In intragroup comparison, there was a statistically significant increase in the width of keratinized tissue in both the groups (*P* = 0.001) between baseline and 1 mo and between 1 mo and 3 mo respectively (*P* = 0.001; *P* = 0.013) (Table 15).

The mean thickness of keratinized tissue observed for the test group were 1.64 ± 0.237 mm, 2.68 ± 0.233 mm, 2.52 ± 0.211 mm, and 2.45 ± 0.252 mm and for the control group were 1.61 ± 0.201 mm, 2.11 ± 0.193 mm, 2.01 ± 0.179 mm, and 1.91 ± 0.166 mm at baseline, 1 mo, 3 mo, and 6 mo, respectively. In intergroup analysis, there was no statistically significant difference found between the mean thickness of keratinized tissue between the two groups at baseline (*P* > 0.05). However, there was a statistically significant difference at 1 mo, 3 mo, and 6 mo, respectively (Table 16 and Figure 4H). In intragroup analysis, there was a statistically significant increase in the thickness of keratinized tissue in both the groups at all time intervals (*P* = 0.001) (Table 17).

In the analysis of the percentage of root coverage for the test sites in which i-PRF with collagen membrane was used for recession coverage, it was found that at 1st postoperative month, about 75% of sites had 100% root coverage, 20% had of sites > 50% root coverage, and only 5% of sites had 50% root coverage. In 3rd postoperative month, 50% of sites had 100% root coverage, 30% had > 50% root coverage, and 20% of sites had 50% root coverage. In the 6th postoperative month, only 25% of sites

Table 7 Intragroup comparison of mean pocket depth scores obtained by using injectable platelet-rich fibrin + collagen membrane and collagen membrane at different time intervals using paired *t* test

i-PRF + CM in mo	mean ± SD	*P* value	CM in mo	mean ± SD	*P* value
0	1.75 ± 0.444	0.001[a]	0	2.05 ± 0.6	0.001[a]
1	2.65 ± 0.489		1	2.8 ± 0.83	
0	1.775 ± 0.444	0.01[a]	0	2.05 ± 0.6	0.002[a]
3	2.05 ± 0.223		3	2.1 ± 0.3	
0	1.75 ± 0.444	1.0	0	2.05 ± 0.6	0.08
6	1.75 ± 0.444		6	1.95 ± 0.223	
1	2.65 ± 0.489	0.001[a]	1	2.8 ± 0.83	0.748
3	2.05 ± 0.223		3	2.1 ± 0.6	
1	2.65 ± 0.489	0.001[a]	1	2.8 ± 0.83	0.428
6	1.75 ± 0.444		6	1.95 ± 0.223	
3	2.45 ± 0.223	0.01[a]	3	2.1 ± 0.3	0.001[a]
6	1.75 ± 0.444		6	1.95 ± 0.223	

[a]$P < 0.01$ statistically significant.
Level of significance at $P < 0.05$. CM: Collagen membrane; i-PRF: Injectable platelet-rich fibrin.

Table 8 Intergroup comparison of mean recession depth scores between injectable platelet-rich fibrin + collagen membrane and collagen membrane at different time intervals using unpaired *t* test

Time (mo)	Group	*n*	mean ± SD	*P* value
0	i-PRF + CM	20	2.7 ± 0.865	0.431
	CM	20	2.9 ± 0.718	NS
1	i-PRF + CM	20	0.25 ± 0.444	0.108
	CM	20	0.5 ± 0.513	NS
3	i-PRF + CM	20	0.5 ± 0.513	0.008[a]
	CM	20	0.95 ± 0.51	
6	i-PRF + CM	20	0.9 ± 0.641	0.04[b]
	CM	20	1.3 ± 0.571	

[a]$P < 0.01$ statistically significant.
[b]$P < 0.05$ statistically significant.
CM: Collagen membrane; i-PRF: Injectable platelet-rich fibrin; NS: Not significant.

remained at 100% root coverage, 25% of sites had > 50% root coverage, 45% of sites had 50% root coverage, and 5% of sites had < 50% root coverage (Figure 5A). While in the analysis of the percentage of root coverage for the control sites in which only collagen membrane was used for recession coverage, it was found that at 1st postoperative month about 50% of sites had 100% root coverage, 40% of sites had > 50% root coverage, and 10% of sites had 50% root coverage. In the 3rd postoperative month, only 15% of sites had 100% root coverage, 55% had > 50% root coverage, 20% of sites had 50% root coverage, and 10% of sites had < 50% of root coverage. In the 6th postoperative month, only 5% of sites remained at 100% root coverage, 30% of sites had > 50% root coverage, 40% of sites had 50% of root coverage, and 25% of sites had < 50% root coverage (Figure 5B).

In the overall percentage of root coverage, it was found that in the test group 91.6%, 81.6%, and 67% root coverage was found at 1 mo, 3 mo, and 6 mo, respectively, while in the control group it was found 82.3%, 66.4%, and 53.95% of root coverage at 1 mo, 3 mo and 6 mo, respectively (Table 18 and Figure 5C).

Table 9 Intragroup comparison of mean recession depth scores obtained by using injectable platelet-rich fibrin + collagen membrane and collagen membrane at different time intervals using paired *t* test

i-PRF + CM in mo	mean ± SD	*P* value	CM in mo	mean ± SD	*P* value
0	2.7 ± 0.86	0.001[a]	0	2.9 ± 0.71	0.001[a]
1	0.25 ± 0.4		1	0.5 ± 0.51	
0	2.7 ± 0.86	0.001[a]	0	2.9 ± 0.71	0.001[a]
3	0.5 ± 0.5		3	0.95 ± 0.51	
0	2.7 ± 0.86	0.001[a]	0	2.9 ± 0.71	0.001[a]
6	0.9 ± 0.64		6	1.3 ± 0.57	
1	0.25 ± 0.4	0.021[b]	1	0.5 ± 0.51	0.001[a]
3	0.5 ± 0.5		3	0.95 ± 0.51	
1	0.025 ± 0.4	0.001[a]	1	0.5 ± 0.51	0.001[a]
6	0.9 ± 0.64		6	1.3 ± 0.57	
3	0.5 ± 0.5	0.002[a]	3	0.95 ± 0.51	0.005[a]
6	0.9 ± 0.64		6	1.3 ± 0.57	

[a]$P < 0.01$ statistically significant.
[b]$P < 0.05$ statistically significant.
Level of significance at $P < 0.05$. CM: Collagen membrane; i-PRF: Injectable platelet-rich fibrin.

Table 10 Intergroup comparison of mean recession width scores between injectable platelet-rich fibrin + collagen membrane and collagen membrane at different time intervals using Mann-Whitney *U* test

Time (mo)	Group	*n*	mean ± SD		*P* value
0	i-PRF + CM	20	3.5	0.607	0.400
	CM	20	3.7	0.733	NS
1	i-PRF + CM	20	0.5	0.889	0.107
	CM	20	1	1.026	NS
3	i-PRF + CM	20	1	1.026	0.080
	CM	20	1.85	0.875	
6	i-PRF + CM	20	1.65	1.04	0.001[a]
	CM	20	2.55	0.759	

[a]$P < 0.01$ statistically significant.
Level of significance at [a]$P < 0.05$. CM: Collagen membrane; i-PRF: Injectable platelet-rich fibrin; NS: Not significant using Mann-Whitney U test.

DISCUSSION

Gingival recession defects present clinicians with significant therapeutic challenges, including restoration of protective anatomy of the mucogingival complex, reestablishment of the aesthetic balance between soft tissues and adjacent tooth structures, and, ideally, regeneration of the lost cementum, periodontal ligament and supporting alveolar bone[18]. Although a wide range of therapeutic alternative exist for treatment of isolated or multiple gingival recessions, according to the available systematic reviews, coronally advanced flap with subepithelial connective tissue graft is the most predictable approach and is considered as the gold standard for root coverage procedures[19-22].

The large avascular area, which usually leads to difficulty in restoring blood supply to the grafted tissue and which is vital for healing, the need for large amount of donor tissue, and the presence of non-carious cervical lesions, which are often associated with multiple gingival recessions, compound the problem[3]. Also, muscle pull during healing often leads to incomplete root coverage or relapse of the recession[4]. Taking all these factors into consideration, the VISTA technique, which is minimally invasive, does not compromise the blood supply, and yet results in improvement of all the clinical

Table 11 Intragroup comparison of mean recession width scores obtained by using injectable platelet-rich fibrin + collagen membrane and collagen membrane at different time intervals using Wilcoxon signed rank test

i-PRF + CM in mo	mean ± SD	*P* value	CM in mo	mean ± SD	*P* value
0	3.5 ± 0.6	0.001[a]	0	3.7 ± 0.73	0.001[a]
1	0.5 ± 0.8		1	1 ± 1.02	
0	3.5 ± 0.6	0.001[a]	0	3.7 ± 0.73	0.001[a]
3	1 ± 1.02		3	1.85 ± 0.85	
0	3.5 ± 0.6	0.001[a]	0	3.7 ± 0.73	0.001[a]
6	1.65 ± 1.03		6	2.55 ± 0.75	
1	0.5 ± 0.8	0.025[b]	1	1 ± 1.02	0.004[a]
3	1 ± 1.02		3	1.85 ± 0.85	
1	0.5 ± 0.8	0.001[a]	1	1 ± 1.02	0.001[a]
6	1.65 ± 1.03		6	2.55 ± 0.75	
3	1 ± 1.02	0.009[a]	3	1.85 ± 0.85	0.001[a]
6	1.65 ± 1.03		6	2.55 ± 0.75	

[a]$P < 0.01$ statistically significant.
[b]$P < 0.05$ statistically significant.
Level of significance at $P < 0.05$. CM: Collagen membrane; i-PRF: Injectable platelet-rich fibrin.

Table 12 Intergroup comparison of mean relative attachment level scores between injectable platelet-rich fibrin + collagen membrane at different time intervals using Mann-Whitney *U* test

Time (mo)	Group	*n*	mean ± SD	*P* value
0	i-PRF + CM	20	7.3 ± 0.801	0.429
	CM	20	7.05 ± 0.826	NS
1	i-PRF + CM	20	5.65 ± 1.348	0.620
	CM	20	5.4 ± 0.94	NS
3	i-PRF + CM	20	5.25 ± 1.293	0.779
	CM	20	5.05 ± 0.945	NS
6	i-PRF + CM	20	5.55 ± 1.099	0.779
	CM	20	5.45 ± 0.826	NS

Level of significance at $P < 0.05$. CM: Collagen membrane; i-PRF: Injectable platelet-rich fibrin; NS: Not significant using Mann-Whitney U test.

parameters, can be considered an accepted approach[3,4].

The advantage of the VISTA technique over other tunneling approaches and classical techniques of gingival augmentation is the degree of coronal advancement of the gingival margin advocated during the procedure[3]. Placement of the initial vertical access incision and the subperiosteal tunnel entrance far from the gingival margin reduces the risk of trauma to the gingiva, while at the same time maintains the integrity of the interdental papilla by avoiding papillary reflection and marginal tissue loss on the teeth being treated[3,5,23]. It also provides a wider access to the surgical region, improves visualization through the single incision with no visible scarring, maximizing the aesthetic outcome[3,6]. The positioning of the gingival margin to the most coronal level of the adjacent interproximal papilla rather than to the cementoenamel junction, with the help of coronally anchored suturing technique on the facial surface of each tooth, effectively minimizes micromotion of the regenerative site and prevents apical relapse of the gingival margin during the initial stages of healing by compensating for some degree of apical migration during the healing period[3].

Dandu *et al*[24] conducted a split mouth randomized controlled trial in 15 patients having bilateral Miller class I and II recession defects. Results revealed mean percentage root coverage of 87.37% + 17.78% with statistically significant gains in the width of keratinized gingiva and a clinical attachment

Table 13 Intragroup comparison of relative attachment level scores obtained by using injectable platelet-rich fibrin + collagen membrane and collagen membrane at different time intervals using Wilcoxon signed rank test

i-PRF + CM in mo	mean ± SD	*P* value	CM in mo	mean ± SD	*P* value
0	7.3 ± 0.8	0.001[a]	0	7.05 ± 0.82	0.001[a]
1	5.6 ± 1.3		1	5.4 ± 0.94	
0	7.3 ± 0.8	0.001[a]	0	7.05 ± 0.82	0.001[a]
3	5.25 ± 1.29		3	5.05 ± 0.94	
0	7.3 ± 0.8	0.001[a]	0	7.05 ± 0.82	0.001[a]
6	5.55 ± 1.09		6	5.45 ± 0.82	
1	5.6 ± 1.3	0.021[b]	1	5.4 ± 0.94	0.124
3	5.25 ± 1.29		3	5.05 ± 0.94	
1	5.6 ± 1.3	0.589	1	5.4 ± 0.94	0.868
6	5.55 ± 1.06		6	5.45 ± 0.82	
3	5.52 ± 1.29	0.06	3	5.05 ± 0.94	0.021[a]
6	5.55 ± 1.06		6	5.45 ± 0.82	

[a]$P < 0.01$ statistically significant.
[b]$P < 0.05$ statistically significant.
Level of significance at $P < 0.05$. CM: Collagen membrane; i-PRF: Injectable platelet-rich fibrin.

Table 14 Intergroup comparison of width of keratinized tissue between injectable platelet-rich fibrin + collagen membrane at different time intervals using Mann-Whitney *U* test

Time (mo)	Group	*n*	mean ± SD	*P* value
0	i-PRF + CM	20	1.6 ± 0.503	0.183
	CM	20	1.35 ± 0.489	NS
1	i-PRF + CM	20	2.85 ± 0.489	0.040[b]
	CM	20	2.45 ± 0.605	
3	i-PRF + CM	20	3.5 ± 0.513	0.004[a]
	CM	20	2.9 ± 0.447	
6	i-PRF + CM	20	3.4 ± 0.598	0.003[a]
	CM	20	2.75 ± 0.444	

[a]$P < 0.01$ statistically significant.
[b]$P < 0.05$ statistically significant.
Level of significance at $P < 0.05$. CM: Collagen membrane; i-PRF: Injectable platelet-rich fibrin; NS: Not significant.

level obtained at 9 mo. Reddy *et al*[8] conducted a case series study to evaluate clinical efficacy of the VISTA technique in combination with PRF and CTG in the treatment of gingival recession defects. Results obtained showed complete root coverage in all the cases at 6 mo and concluded that the VISTA technique overcomes the shortcoming of other treatment options and gives better results for multiple gingival recession defects. Garg *et al*[10] evaluated the efficacy of VISTA with or without PRF membrane in the treatment of multiple Millers class I and class II gingival recession defects. One hundred percent coverage was obtained in class I sites treated with VISTA approach with or without PRF-membrane. Millers class II recession defects showed 100% coverage with 80%-85% of CAL gain at site treated with VISTA + PRF membrane as compared to sites treated with VISTA technique, which only displayed 50% coverage. They concluded that the VISTA technique alone is a successful approach for the treatment of class-I and II multiple recession defects. Moreover, along with PRF-membrane, the VISTA technique has proven efficiency for treatment of class - III recession defects. Mansouri *et al*[5] compared the clinical efficacy of the VISTA technique with CTG *vs* CAF with CTG for the treatment of multiple gingival recession defects. Results revealed a significant decrease in recession depth, recession width, and clinical

Table 15 Intragroup comparison of width of keratinized tissue scores obtained by using injectable platelet-rich fibrin + collagen membrane and collagen membrane at different time intervals using Wilcoxon signed rank test

i-PRF + CM in mo	mean ± SD	*P* value	CM in mo	mean ± SD	*P* value
0	1.6 ± 0.5	0.001[a]	0	1.35 ± 0.48	0.001[a]
1	2.85 ± 0.48		1	2.45 ± 0.6	
0	1.6 ± 0.5	0.001[a]	0	1.35 ± 0.48	0.001[a]
3	3.5 ± 0.51		3	2.9 ± 0.44	
0	1.6 ± 0.5	0.001[a]	0	1.35 ± 0.48	0.001[a]
6	3.4 ± 0.59		6	2.75 ± 0.44	
1	2.85 ± 0.48	0.001[a]	1	2.45 ± 0.6	0.001[a]
3	3.5 ± 0.51		3	2.9 ± 0.44	
1	2.85 ± 0.48	0.001[a]	1	2.45 ± 0.6	0.001[a]
6	3.4 ± 0.59		6	2.75 ± 0.44	
3	3.5 ± 0.51	0.001[a]	3	2.9 ± 0.44	0.001[a]
6	3.4 ± 0.59		6	2.75 ± 0.44	

[a]$P < 0.01$ statistically significant.
Level of significance at $P < 0.05$. CM: Collagen membrane; i-PRF: Injectable platelet-rich fibrin.

Table 16 Intergroup comparison of thickness of keratinized tissue scores between injectable platelet-rich fibrin + collagen membrane and collagen membrane at different time intervals using unpaired *t* test

Time (mo)	Group	*n*	mean ± SD	*P* value
0	i-PRF + CM	20	1.65 ± 0.238	0.685
	CM	20	1.62 ± 0.202	NS
1	i-PRF + CM	20	2.69 ± 0.233	0.001[a]
	CM	20	2.12 ± 0.193	
3	i-PRF + CM	20	2.53 ± 0.212	0.001[a]
	CM	20	2.02 ± 0.18	
6	i-PRF + CM	20	2.46 ± 0.252	0.001[a]
	CM	20	1.91 ± 0.166	

[a]$P < 0.01$ statistically significant using unpaired *t* test.
Level of significance at $P < 0.05$; CM: Collagen membrane; i-PRF: Injectable platelet-rich fibrin; NS: Not significant.

attachment level, and an increase in keratinized tissue width in both the groups. It was concluded that VISTA, as a minimally invasive approach, was able to treat gingival recession defects and reduce their height and width, yielding results similar to those obtained by the use of CAF, which is the gold standard procedure for root coverage. Mohamed *et al*[6] compared the Tunnel technique with the VISTA technique for the treatment of multiple gingival recessions with ADM. The percentage of root coverage between VISTA + ADM sites and tunnel + ADM sites was statistically significant in favor of VISTA + ADM. They concluded that an ADM allograft can be recommended as an alternative to connective tissue graft, but its combination with the VISTA technique is found to be more efficient than tunnel + ADM in treatment of Miller class I and II multiple gingival recessions and lead to more favorable root coverage.

Guided tissue regeneration is a reliable method for periodontal regeneration and the introduction of resorbable collagen membranes allowed clinicians to achieve a predictable, new connective tissue attachment over the exposed root surface[25-29]. Collagen membrane, acting as a barrier, mechanically prevents the epithelial cell migration during the initial stages of healing, allowing the regeneration of the treated root surface by connective tissue cells, eventually leading to the development of a new connective tissue attachment. The cross-linked structure slows the degradation rate, allowing the

Table 17 Intragroup comparison of thickness of keratinized tissue scores obtained by using injectable platelet-rich fibrin and collagen membrane at different time intervals using paired *t* test

i-PRF + CM in mo	mean ± SD	*P* value	CM in mo	mean ± SD	*P* value
0	1.64 ± 0.237	0.001[a]	0	1.61 ± 0.201	0.001[a]
1	2.68 ± 0.233		1	2.11 ± 0.193	
0	1.64 ± 0.237	0.001[a]	0	1.61 ± 0.201	0.001[a]
3	2.52 ± 0.211		3	2.01 ± 0.179	
0	1.64 ± 0.237	0.001[a]	0	1.61 ± 0.201	0.001[a]
6	2.45 ± 0.252		6	1.91 ± 0.166	
1	2.68 ± 0.233	0.001[a]	1	2.11 ± 0.193	0.001[a]
3	2.52 ± 0.211		3	2.01 ± 0.179	
1	2.68 ± 0.233	0.001[a]	1	2.11 ± 0.193	0.001[a]
6	2.45 ± 0.252		6	1.91 ± 0.166	
3	2.52 ± 0.211	0.001[a]	3	2.01 ± 0.179	0.001[a]
6	2.45 ± 0.252		6	1.91 ± 0.166	

[a]$P < 0.01$ statistically significant.

Level of significance at $P < 0.05$. CM: Collagen membrane; i-PRF: Injectable platelet-rich fibrin.

Table 18 Overall percentage of root coverage in the 1st month, 3rd month and 6th month in patients treated with injectable platelet-rich fibrin + collagen membrane and collagen membrane respectively

Group	Month 1	Month 3	Month 6
i-PRF + CM	91.6	81.6	67
CM	82.3	66.4	53.95

CM: Collagen membrane; i-PRF: Injectable platelet-rich fibrin.

membrane to remain in the site for a sufficient period of time which prevents the apical migration of epithelial cells in late stages of healing, thus discouraging the formation of long junctional epithelial attachment and favoring the development of a connective tissue attachment[30,31].

Since the introduction of PRF[32], it has been used in various types of periodontal defects with good results. PRF is autologous, easy to prepare in a short period of time, and has little biochemical handling, giving it an advantage over other techniques. It has a matrix of fibrin, which has trapped platelets, leukocytes, and cytokines. It acts as a source of growth factors, which are released slowly over a period of 7 d and play an important role in recession coverage[33]. One drawback that limits the applications of PRF is that PRF is currently available only in a gel form, which is not conducive to being injected[34-36].

i-PRF also has similar properties as PRF; however, it is available in injectable form. It contains all components of PRF, including platelets, white blood cells, and all the clotting factors comprising fibrinogen in an uncoagulated form[37]. The major advantages of i-PRF over other platelet concentrates is that it contains a greater number of regenerative cells with higher concentrations of growth factors and leukocytes due to the "slow speed concept" of blood centrifugation[38,39]. Leukocytes have been known to play an important role in wound healing and tissue regeneration. With the increased number of these cells available, this possibly increases the release of growth factors like platelet-derived growth factor (PDGF), epidermal growth factor, transforming growth factor-β (TGF-β), and insulin-like growth factor-1[40,41].

According to Miron *et al*[16] when i-PRF was compared with PRP in terms of cell proliferation, PRP was more effective than injectable PRF. However, injectable PRF demonstrated significantly better results than PRP did, including cell migration and messenger ribonucleic acid expression of TGF-β, PDGF, and collagen type 1a2 at both 3- and 7-d intervals. Also, whereas PRP had completely dissolved over a period of 10 d, injectable PRF formed a small clot as a dynamic gel and maintained release of growth factor for over 10 d. Varela *et al*[42] observed that i-PRF induces higher cell migration and expression of TGF-β, PDGF, and type I collagen, which stimulates the differentiation of osteoblasts and deposits a mineral matrix. İzol *et al*[43] investigated the outcome of i-PRF on root coverage of free

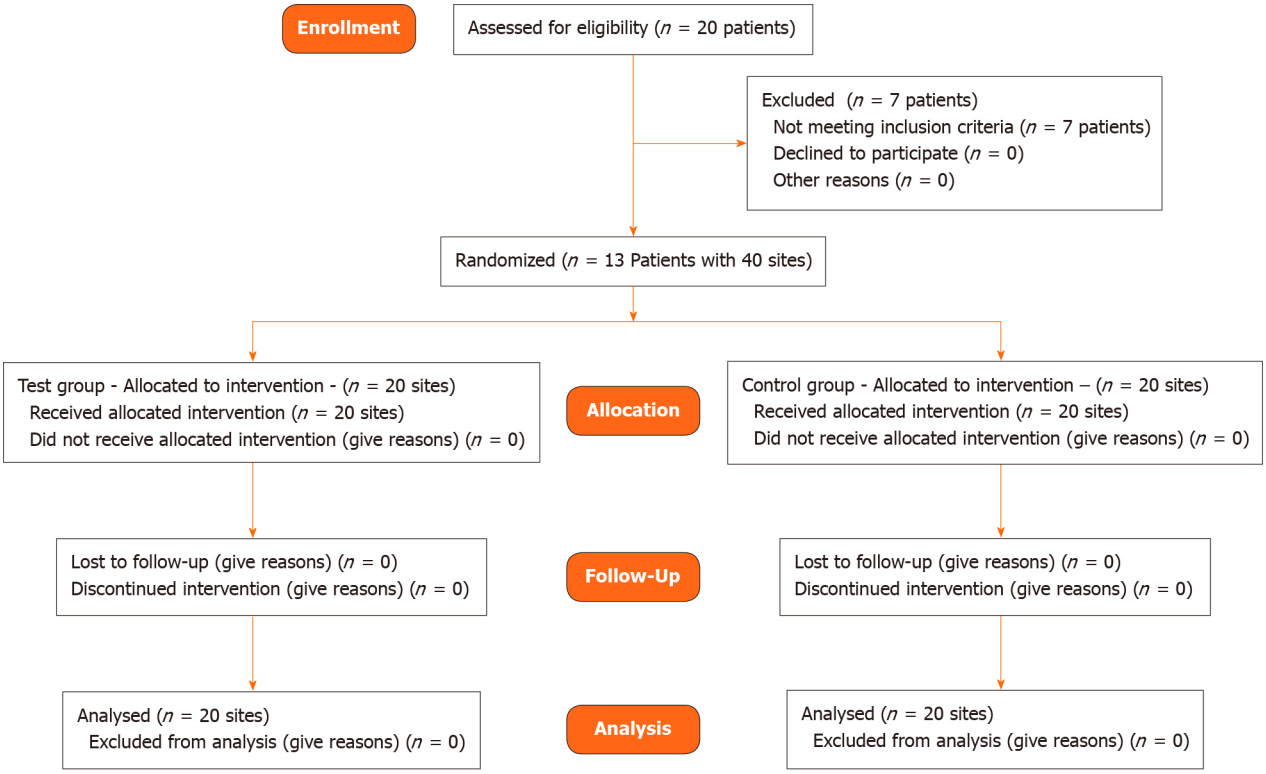

DOI: 10.5493/wjem.v12.i4.68

Figure 3 CONSORT flow diagram.

gingival graft surgery. The result showed a positive effect on the coverage of the root surface. Ucak Turer *et al*[44] investigated the combined effect of SCTG with i-PRF and SCTG alone in a coronally positioned flap procedure for the treatment of root coverage and observed that the combined effect of SCTG and i-PRF achieved a greater keratinized tissue width and showed predictable results in reduced gingival recession. Ozsagir *et al*[45] evaluated the efficacy of i-PRF alone and in combination with microneedling on gingival thickness and KTW in patients with a thin biotype. They stated that microneedling has a beneficial result on the augmentation of gingival thickness. Al-Maawi *et al*[46] analyzed the combination of an autologous i-PRF matrix as a drug delivery system, with five different xenogeneic collagen-based biomaterials (Mucograft®, Bio-Gide®, Mucoderm®, Collprotect® and BEGO®) histologically. They found that i-PRF could be used as a drug delivery system to support GTR/GBR and enhance their biomaterial bioactivity. Chai *et al*[47] conducted a comparative analysis study to compare the cellular regenerative activity of human dental pulp cells (hDPCs) when cultured with either i-PRF or traditional PRP. The findings from the study suggested that i-PRF promoted higher regeneration potential of hDPCs when compared with traditional PRP. Furthermore, i-PRF also reduced the inflammatory condition created by lipopolsacharrides and maintained a supportive regenerative ability for stimulation of odontoblastic differentiation and reparative dentin in hDPCs. Bennardo *et al*[48] conducted a split mouth randomized controlled trial to compare the efficacy of i-PRF and triamcinolone acetonide (TA) injective therapies in patients with symptomatic oral lichen planus (OLP). The results obtained with i-PRF are similar to those obtained with TA. It was concluded that although i-PRF injections do not represent a standard treatment option, they have proved to be equally effective in reducing symptoms and dimensions of OLP lesions.

The VISTA technique has been applied for gingival recession coverage using different regenerative materials like CTG[5,49,50], PRF[50,51], titanium PRF[51], ADM[6], GEM 21S[24], recombinant human platelet derived growth factor[4], and collagen membrane[52]; however, there was no study using i-PRF in combination with collagen membrane using VISTA technique for recession coverage.

In this split mouth randomized clinical trial, the full mouth plaque and gingival index scores remained low throughout the study period. It was observed that plaque and gingival index were increased in 1 mo, which could be due to the coronally advanced suture held in the facial enamel surface for 3 wk postoperatively leading to a difficulty in maintaining oral hygiene in the operated region. There was a reduction in the plaque and gingival indexes at the 3rd and 6th postoperative month, which is due to better patient compliance and regular oral hygiene instructions given to the patients, thereby enabling improved plaque control efficiency.

The change in mean probing depth in i-PRF with collagen membrane group was statistically insignificant between both groups, which is in accordance with observation by Geeti *et al*[53] Similarly, another study done by Mohamed *et al*[6] where they used acellular dermal matrix (ADM) for recession coverage

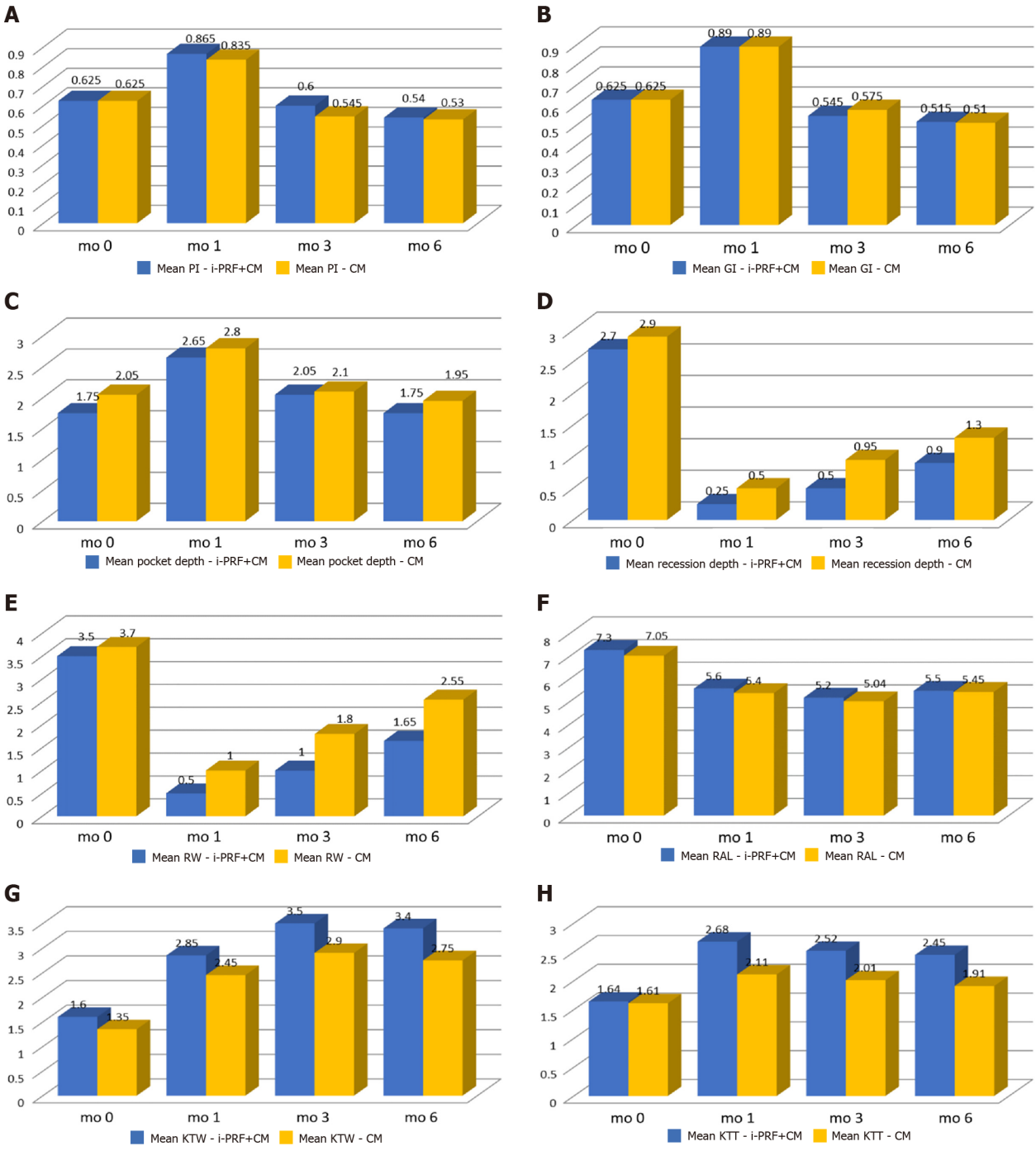

DOI: 10.5493/wjem.v12.i4.68

Figure 4 Comparison of injectable platelet-rich fibrin + collagen membrane and collagen membrane at different time intervals. A: Comparison of mean plaque index (PI) scores; B: Comparison of mean gingival index (GI) scores; C: Comparison of mean pocket depth (PD) scores; D: Comparison of mean recession depth (RD) scores; E: Comparison of mean recession width (RW) scores; F: Comparison of mean relative attachment level (RAL) scores; G: Comparison of mean keratinized tissue width (KTW) scores; H: Comparison of mean keratinized tissue thickness (KTT) scores. CM: Collagen membrane; i-PRF: Injectable platelet-rich fibrin; PI: Plaque index; mo: Month.

showed reduction in probing depth score. The intergroup comparison in the present study was statistically insignificant at each time intervals which is in accordance with the study done by Subbareddy *et al* [3].

Recession depth in the present study revealed a significant reduction of the test and control groups at the end of 6 mo postoperatively. This is similar with the case series done by Raja Rajeswari *et al*[54] There was a significant difference in the intergroup comparison at 3 mo and 6 mo, which is in line with the split mouth study done by Subbareddy *et al*[3] in which VISTA + PRF was compared with VISTA + SCTG.

Reduction in recession width was statistically significant in each postoperative visit in comparison to baseline for both the groups. This is in agreement with the study done by Mansouri *et al*[5] in which

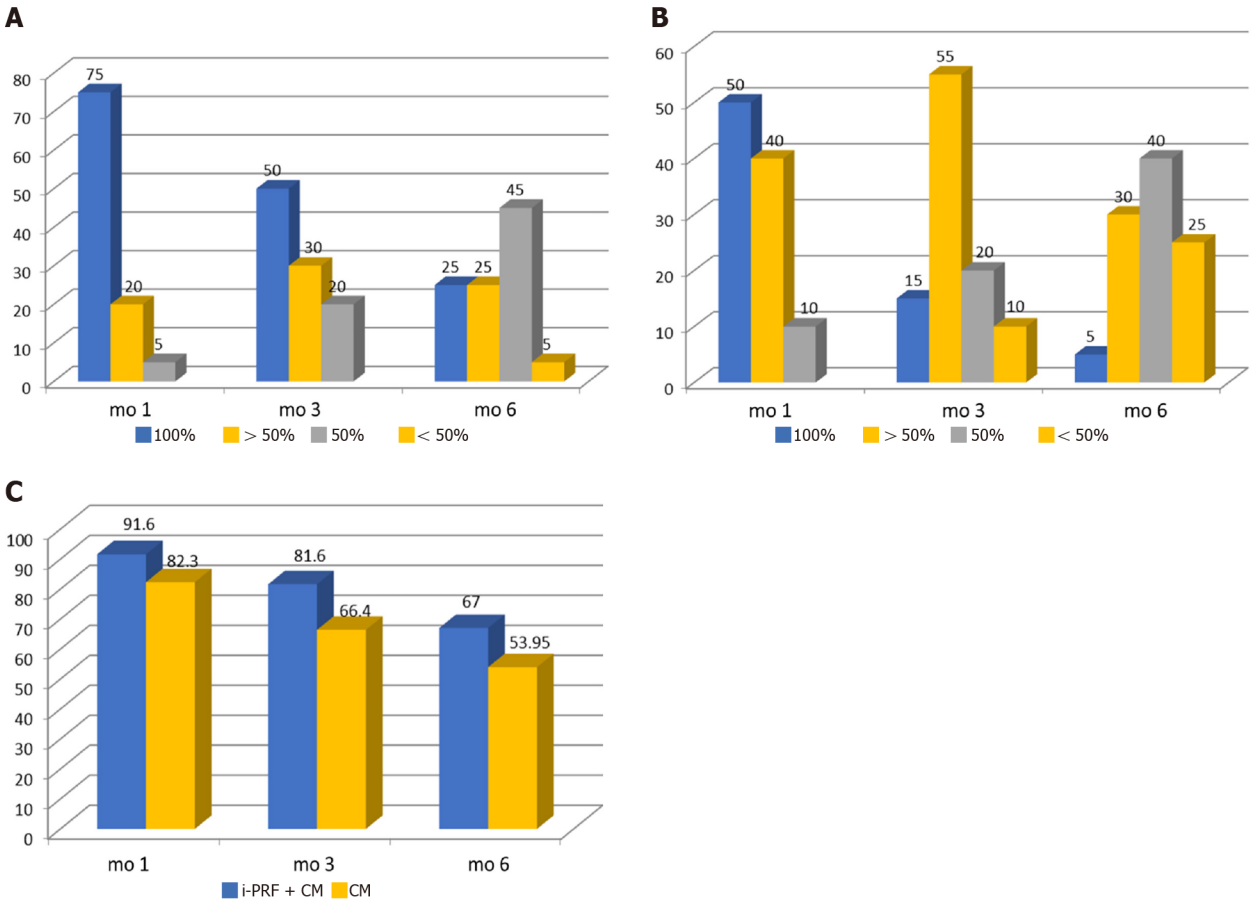

DOI: 10.5493/wjem.v12.i4.68

Figure 5 Percentage of root coverage. A: Injectable platelet-rich fibrin (i-PRF) + collagen membrane (CM) group (in percentage); B: CM group (in percentages); C: Following treatment with i-PRF + CM and CM. mo: Month.

VISTA was compared with coronally advanced flap procedure using connective tissue graft. The present study shows i-PRF with collagen membrane is equally effective in reducing the width of a recession when compared to VISTA with CTG.

There was a significant increase in attachment gain level for both i-PRF + CM and CM groups at 6 mo, which is in accordance with Mansouri *et al*[5]. Improvement in clinical attachment may be because of recession coverage that results from coronal shift of attachment apparatus during coronally advance flap procedures.

In the present study, the width of keratinized gingiva in the subjects of both groups showed significant increase in 1 mo and 3 mo, and it was sustained at least until 6 mo. These results are in accordance with study done by Mohamed *et al*[6], though the study used VISTA + PRF for recession coverage. Similarly, a study done by Dandu *et al*[24] showed gain in width of keratinized gingiva in which VISTA with collagen membrane enhanced with GEM 21S was used for recession coverage.

There was a significant gain in the mean thickness of keratinized gingiva in both the test and control groups, which is similar to the results of study using VISTA with PRF done by Geeti *et al*[53] and Raja Rajeswari *et al*[54].

In the overall percentage of root coverage of the present study, it was observed that at 1 mo there was 91% and 82% of root coverage, which reduced to 67% and 53% of root coverage at 6 mo for test and control groups, respectively. It was also observed that at the end of 6 mo, 25% (5) of the sites had complete root coverage for test group while only 5% (1) of the sites had complete root coverage for control group. Similarly, in the study by Mansouri *et al*[5], mean root coverage achieved was 70.69%, with 50% of cases having complete root coverage in the VISTA with CTG group. A study done by Subbareddy *et al*[3] showed that in the test group involving VISTA with PRF, 30.33% of sites obtained complete root coverage, whereas the remaining sites constituting 69.67% partial root coverage.

In the overall assessment of the results of the study, it was observed that probing depth, recession depth, recession width, and the relative attachment level, both the test and control sites had similar results. Width of keratinized tissue, thickness of keratinized tissue, and the percentage of root coverage in i-PRF with collagen membrane had better results than sites where only collagen membrane was used for recession coverage. This can be attributed to the VISTA technique, as it was a minimally invasive surgery which not only reduces the trauma to the operating site, but also preserves the major blood

vessels of the flap and blood supply to the area, resulting in better nourishment of the collagen membrane.

The use of i-PRF is not only helpful for enrichment of the collagen membrane with various growth factors responsible for tissue regeneration, but also injecting it into the mesial and distal aspects into periodontal ligament and into the facial aspects of gingiva is an added benefit for stimulation of wound healing[55].

This study must be interpreted with consideration of relatively small sample size (13 subjects) and the shorter study duration (6 mo).

CONCLUSION

Based on the results of the study it can be concluded that the use of the minimally invasive VISTA technique, along with a collagen membrane acting as scaffold and chemoattractant with the added benefit of an injectable form of PRF with the capacity of releasing more growth factors and regenerative cells responsible for tissue regeneration, can be successfully used as a treatment method for multiple or isolated gingival recessions of Miller's class-I and class-II defects though further multicentric longitudinal studies are needed to be carried out to validate to the results of the present study.

ARTICLE HIGHLIGHTS

Research background

Gingival recession is being treated using various therapeutic approaches with varying degrees of success depending on the etiology and treatment approach. Among them, coronally advanced flap technique with a connective tissue graft is considered the gold standard for soft tissue augmentation and periodontal root coverage. However, this technique has some disadvantages, including harvesting from a donor site, limited tissue availability, and increased potential for post-harvesting morbidity. With the introduction of the minimally invasive vestibular incision subperiosteal tunnel access (VISTA) technique, similar results could be obtained. It tries to preserve the interdental papillae and unhampered blood supply while maintaining the marginal integrity and minimizing the micromotion of flap for faster wound healing with no visible scarring to maximize the aesthetic outcome. This study is an attempt to find the efficacy of the VISTA technique using collagen membrane soaked in autologous injectable formulation of platelet-rich fibrin, termed as injectable platelet-rich fibrin (i-PRF) for the treatment of multiple gingival recession coverage.

Research motivation

The main topic is to compare the efficacy of minimally invasive VISTA technique for the treatment of multiple gingival recession coverage using a collagen membrane or a collagen membrane soaked in i-PRF. Placement of the initial vertical access incision and the subperiosteal tunnel entrance being far from the gingival margin reduces the risk of trauma to the gingiva, while at the same time maintaining the integrity of the interdental papilla by avoiding papillary reflection and marginal tissue loss of the teeth being treated. It also provides wider access to the surgical region and improves visualization through a single incision with no visible scarring, maximizing the aesthetic outcome. The positioning of the gingival margin to the most coronal level of the adjacent interproximal papilla rather than to the cementoenamel junction, with the help of the coronally anchored suturing technique on the facial surface of each tooth, effectively minimizes micromotion of the regenerative site and prevents apical relapse of the gingival margin during the initial stages of healing. The use of i-PRF also has similar properties as PRF, but has the added benefit of being available in an injectable form. It contains all components of PRF, including platelets, white blood cells, and all the clotting factors comprising fibrinogen in an uncoagulated form, making them readily available. The major advantage of i-PRF over other platelet concentrates is that it contains a greater number of regenerative cells with higher concentrations of growth factors and leukocytes. With the increased number of cells, there is possibly an increased release of growth factors like platelet-derived growth factor, epidermal growth factor, transforming growth factor and insulin-like growth factor-1.

Research objectives

The main objective is to compare the efficacy of the VISTA technique incorporating collagen membrane alone with the VISTA technique with collagen membrane soaked in injectable platelet-rich fibrin for gingival recession coverage in terms of clinical parameters like pocket depth, recession width, recession depth, width of keratinized gingiva, thickness of keratinized tissue, and the percentage of root coverage. In the overall assessment of the result of the study, it was observed that probing depth, recession depth, recession width, and relative attachment level are similar between the test and control sites. However, the width of keratinized tissue, the thickness of keratinized tissue, and the percentage of root coverage

had better results for sites treated with i-PRF than sites where only collagen membrane was used for recession coverage. This can be attributed to the VISTA technique as it was a minimally invasive surgery, which not only reduces the trauma to the operating site, but also preserves the major blood vessels of the flap and blood supply to the area, resulting in better nourishment of the collagen membrane. The use of i-PRF is not only helpful for the enrichment of collagen membrane with various growth factors responsible for tissue regeneration, but also injecting it into the mesial and distal aspects of periodontal ligament and into the facial aspects of gingiva is an added benefit for stimulation of wound healing.

Research methods

The data was analyzed using SPSS Ver 22 for windows, (IBM Corp, Armonik, United States). Descriptive statistics were expressed as a mean with standard deviations and proportions. Normally distributed data were analyzed using a paired *t*-test for intragroup comparison and an unpaired *t*-test for intergroup comparison. Skewed data were analyzed using the Wilcoxon signed rank test for intragroup and Mann-Whitney *U* test for intergroup comparison. The level of significance was set at $P < 0.05$.

Research results

The result of the study observed that probing depth, recession depth, recession width, and relative attachment level are similar in test sites compared with control sites. However, the width of keratinized tissue, the thickness of keratinized tissue, and the percentage of root coverage had better results in sites treated with i-PRF with collagen membrane than sites where only collagen membrane was used for recession coverage. This can be attributed to the VISTA technique, as it is a minimally invasive surgery which not only reduces the trauma to the operating site, but also preserves the major blood vessels of the flap and blood supply to the area, resulting in better nourishment of the collagen membrane. The use of i-PRF is not only helpful for the enrichment of collagen membrane with various growth factors responsible for tissue regeneration, but also injecting it into the mesial and distal aspects of periodontal ligament and into the facial aspects of gingiva is an added benefit for stimulation of wound healing.

Research conclusions

The VISTA technique has been applied for gingival recession coverage using different regenerative materials like connective tissue graft, PRF, titanium PRF, acellular dermal matrix, GEM 21S, recombinant human platelet derived growth factor, and collagen membrane; however, there was no study using i-PRF in combination with collagen membrane using VISTA technique for gingival recession coverage. The results of the study proposed that the use of minimally invasive VISTA technique, along with collagen membrane with the added benefit of the injectable form of platelet-rich fibrin have the capacity of releasing more growth factors and regenerative cells responsible for tissue regeneration, can be successfully used as a treatment method for multiple or isolated gingival recessions of Miller's class-I and class-II defects.

Research perspectives

This study must be interpreted with consideration of the relatively small sample size (13 subjects) and shorter study duration (6 mo). A long term follow-up study with larger sample size is required.

FOOTNOTES

Author contributions: Raj SC, Patra L, Mohanty D, and Katti N contributed to the conceptualization; Patra L, Pradhan SS, Tabassum S, and Mishra AK contributed to the formal analysis and investigations; Mahapatra A and Patnaik K contributed to the methodology; Raj SC contributed to the project administration; Raj SC and Patra L contributed to the writing-original draft; Raj SC, Patra L, Mahapatra A, and Patnaik K contributed to the writing, review, and editing.

Institutional review board statement: The study was recommended by the Institutional Ethics Committee (IEC), under IEC/SCBDCH/049/20189 dated 17/09/2019 before its commencement and was conducted in accordance with the declaration of Helsinki of 1975, as revised in 2000.

Clinical trial registration statement: The study was prospectively registered with clinical trials registry (CTRI/2020/06/026141).

Conflict-of-interest statement: No conflict of interest.

Data sharing statement: Technical appendix, statistical code, and dataset available from the corresponding author at drsubash007@gmail.com. Participants gave informed consent for data sharing.

Country/Territory of origin: India

ORCID number: Laxmikanta Patra 0000-0002-1727-2673; Subash Chandra Raj 0000-0003-2478-077x; Neelima Katti 0000-0001-5551-8702; Devapratim Mohanty 0000-0002-5768-0962; Shib Shankar Pradhan 0000-0003-2479-8072; Shaheda Tabassum 0000-0003-2049-7133; Asit Kumar Mishra 0000-0001-6012-7984; Kaushik Patnaik 0000-0001-8928-6751; Annuroopa Mahapatra 0000-0002-1550-8312.

S-Editor: Zhang H
L-Editor: Filipodia CL
P-Editor: Li X

REFERENCES

1 **Tugnait A**, Clerehugh V. Gingival recession-its significance and management. *J Dent* 2001; **29**: 381-394 [PMID: 11520586 DOI: 10.1016/s0300-5712(01)00035-5]
2 **Niswade G**. Paripex- Gingival recession-a stigma to the tooth. *Indian J Res* 2017; **3**: 72-75
3 **Subbareddy BV**, Gautami PS, Dwarakanath CD, Devi PK, Bhavana P, Radharani K. Vestibular Incision Subperiosteal Tunnel Access Technique with Platelet-Rich Fibrin Compared to Subepithelial Connective Tissue Graft for the Treatment of Multiple Gingival Recessions: A Randomized Controlled Clinical Trial. *Contemp Clin Dent* 2020; **11**: 249-255 [PMID: 33776351 DOI: 10.4103/ccd.ccd_405_19]
4 **Zadeh HH**. Minimally invasive treatment of maxillary anterior gingival recession defects by vestibular incision subperiosteal tunnel access and platelet-derived growth factor BB. *Int J Periodontics Restorative Dent* 2011; **31**: 653-660 [PMID: 22140667]
5 **Dutta S**, Nasim F, Pal D, Singh MK, Chakrabarty H. A novel approach of treating gingival recession by Vestibular Incision Subperiosteal Tunnel Access along with palatal connective tissue graft. *IP Int J Periodontol Implantol* 2020; **5**: 37-40 [DOI: 10.18231/j.ijpi.2020.009]
6 **Mansouri SS**, Moghaddas O, Torabi N, Katayoun Ghafari. Vestibular incisional subperiosteal tunnel access vs coronally advanced flap with connective tissue graft for root coverage of Miller's class I and II gingival recession: A randomized clinical trial. *J Adv Periodontal Implant Dent* 2019; **11**: 12-20 [DOI: 10.15171/japid.2019.003]
7 **Mohamed A**, Marssafy L. Comparative clinical study between Tunnel and VISTA approaches for the treatment of multiple gingival recessions with acellular dermal matrix allograft. *Egypt Dent J* 2020; **66**: 247-259 [DOI: 10.21608/edj.2020.77540]
8 **Reddy S**, Prasad MGS, Bhowmik N, Singh S, Pandit HR, Vimal SK. Vestibular incision subperiosteal tunnel access (VISTA) with platelet-rich fibrin (PRF) and connective tissue graft (CTG) in the management of multiple gingival recession- A case series. *Int J Appl Dent Sci* 2016; **2**: 34-37
9 **Kimble KM**, Eber RM, Soehren S, Shyr Y, Wang HL. Treatment of gingival recession using a collagen membrane with or without the use of demineralized freeze-dried bone allograft for space maintenance. *J Periodontol* 2004; **75**: 210-220 [PMID: 15068108 DOI: 10.1902/jop.2004.75.2.210]
10 **Garg S**, Arora SA, Chhina S, Singh P. Multiple Gingival Recession Coverage Treated with Vestibular Incision Subperiosteal Tunnel Access Approach with or without Platelet-Rich Fibrin - A Case Series. *Contemp Clin Dent* 2017; **8**: 464-468 [PMID: 29042736 DOI: 10.4103/ccd.ccd_142_17]
11 **Dohan DM**, Choukroun J, Diss A, Dohan SL, Dohan AJ, Mouhyi J, Gogly B. Platelet-rich fibrin (PRF): a second-generation platelet concentrate. Part I: technological concepts and evolution. *Oral Surg Oral Med Oral Pathol Oral Radiol Endod* 2006; **101**: e37-e44 [PMID: 16504849 DOI: 10.1016/j.tripleo.2005.07.008]
12 **Dohan DM**, Choukroun J, Diss A, Dohan SL, Dohan AJ, Mouhyi J, Gogly B. Platelet-rich fibrin (PRF): a second-generation platelet concentrate. Part II: platelet-related biologic features. *Oral Surg Oral Med Oral Pathol Oral Radiol Endod* 2006; **101**: e45-e50 [PMID: 16504850 DOI: 10.1016/j.tripleo.2005.07.009]
13 **Dohan DM**, Choukroun J, Diss A, Dohan SL, Dohan AJ, Mouhyi J, Gogly B. Platelet-rich fibrin (PRF): a second-generation platelet concentrate. Part III: leucocyte activation: a new feature for platelet concentrates? *Oral Surg Oral Med Oral Pathol Oral Radiol Endod* 2006; **101**: e51-e55 [PMID: 16504851 DOI: 10.1016/j.tripleo.2005.07.010]
14 **Choukroun J**, Diss A, Simonpieri A, Girard MO, Schoeffler C, Dohan SL, Dohan AJ, Mouhyi J, Dohan DM. Platelet-rich fibrin (PRF): a second-generation platelet concentrate. Part IV: clinical effects on tissue healing. *Oral Surg Oral Med Oral Pathol Oral Radiol Endod* 2006; **101**: e56-e60 [PMID: 16504852 DOI: 10.1016/j.tripleo.2005.07.011]
15 **Jain V**, Triveni MG, Kumar AB, Mehta DS. Role of platelet-rich-fibrin in enhancing palatal wound healing after free graft. *Contemp Clin Dent* 2012; **3**: S240-S243 [PMID: 23230372 DOI: 10.4103/0976-237X.101105]
16 **Miron RJ**, Fujioka-Kobayashi M, Hernandez M, Kandalam U, Zhang Y, Ghanaati S, Choukroun J. Injectable platelet rich fibrin (i-PRF): opportunities in regenerative dentistry? *Clin Oral Investig* 2017; **21**: 2619-2627 [PMID: 28154995 DOI: 10.1007/s00784-017-2063-9]
17 **Agrawal DR**, Jaiswal PG. Injectable Platelet Rich Fibrin (i-PRF): A Gem in Dentistry. *Int J Cur Res Rev* 2020; **12**: 25-30 [DOI: 10.31782/IJCRR.2020.122116]
18 **Rutuja PK**, Lisa C, Rakhewar PS. The vestibular incision subperiosteal tunnel access (VISTA) for treatment of maxillary

anterior gingival recession defects- a case report. *Int J Health Sci Res* 2017; **7**: 360-365

19 **Buti J**, Baccini M, Nieri M, La Marca M, Pini-Prato GP. Bayesian network meta-analysis of root coverage procedures: ranking efficacy and identification of best treatment. *J Clin Periodontol* 2013; **40**: 372-386 [PMID: 23346965 DOI: 10.1111/jcpe.12028]

20 **Cairo F**, Nieri M, Pagliaro U. Efficacy of periodontal plastic surgery procedures in the treatment of localized facial gingival recessions. A systematic review. *J Clin Periodontol* 2014; **41** Suppl 15: S44-S62 [PMID: 24641000 DOI: 10.1111/jcpe.12182]

21 **Moghaddas H**, Esfahanian V, Moghaddas O. Efficacy of subepithelial connective tissue grafts in the treatment of Miller's Class I and II gingival recessions. *J Isfahan Dent Sch* 2011; **7**: 337-353

22 **Roccuzzo M**, Bunino M, Needleman I, Sanz M. Periodontal plastic surgery for treatment of localized gingival recessions: a systematic review. *J Clin Periodontol* 2002; **29** Suppl 3: 178-94; discussion 195 [PMID: 12787218 DOI: 10.1034/j.1600-051x.29.s3.11.x]

23 **Chatterjee A**, Sharma E, Gundanavar G, Subbaiah SK. Treatment of multiple gingival recessions with vista technique: A case series. *J Indian Soc Periodontol* 2015; **19**: 232-235 [PMID: 26015680 DOI: 10.4103/0972-124X.145836]

24 **Dandu SR**, Murthy KR. Multiple Gingival Recession Defects Treated with Coronally Advanced Flap and Either the VISTA Technique Enhanced with GEM 21S or Periosteal Pedicle Graft: A 9-Month Clinical Study. *Int J Periodontics Restorative Dent* 2016; **36**: 231-237 [PMID: 26901301 DOI: 10.11607/prd.2533]

25 **Cortellini P**, Clauser C, Prato GP. Histologic assessment of new attachment following the treatment of a human buccal recession by means of a guided tissue regeneration procedure. *J Periodontol* 1993; **64**: 387-391 [PMID: 8515369 DOI: 10.1902/jop.1993.64.5.387]

26 **Paolantonio M**. Treatment of gingival recessions by combined periodontal regenerative technique, guided tissue regeneration, and subpedicle connective tissue graft. A comparative clinical study. *J Periodontol* 2002; **73**: 53-62 [PMID: 11846201 DOI: 10.1902/jop.2002.73.1.53]

27 **Al-Hamdan K**, Eber R, Sarment D, Kowalski C, Wang HL. Guided tissue regeneration-based root coverage: meta-analysis. *J Periodontol* 2003; **74**: 1520-1533 [PMID: 14653400 DOI: 10.1902/jop.2003.74.10.1520]

28 **Kapare K**, Gopalakrishnan D, Kathariya R, Tyagi T, Bagwe S. Evaluation of efficacy of a novel resorbable collagen membrane for root coverage of Miller's Class I and Class II recession in the maxillary anteriors and premolars. *J Indian Soc Periodontol* 2016; **20**: 520-524 [PMID: 29242688 DOI: 10.4103/0972-124X.207051]

29 **Yuan KH**, Kun LH. Systematic Review of the Clinical Performance of Connective Tissue Graft and Guided Tissue Regeneration in the Treatment of Gingival Recessions of Miller's Classification Grades I and II. *J Exp Clin Med* 2010; **2**: 63-71 [DOI: 10.1016/S1878-3317(10)60011-3]

30 **Wang HL**, Al-Shammari KF. Guided tissue regeneration-based root coverage utilizing collagen membranes: technique and case reports. *Quintessence Int* 2002; **33**: 715-721 [PMID: 12553614]

31 **Wang HL**, O'Neal RB, Thomas CL, Shyr Y, MacNeil RL. Evaluation of an absorbable collagen membrane in treating Class II furcation defects. *J Periodontol* 1994; **65**: 1029-1036 [PMID: 7853126 DOI: 10.1902/jop.1994.65.11.1029]

32 **Choukroun J**, Adda F, Schoeffer C, Vervelle A. The opportunity in perio-implantology: The PRF. *Implantodontie* 2000; **42**: 55-62

33 **Chandran P**, Sivadas A. Platelet-rich fibrin: Its role in periodontal regeneration. *Saudi J Dent Res* 2013; **5**: 1-6 [DOI: 10.1016/j.ksujds.2013.09.001]

34 **Saini K**, Chopra P, Sheokand V. Journey of Platelet Concentrates: A Review. *Biomed Pharmacol J* 2020; **13**: 185-191 [DOI: 10.13005/bpj/1875]

35 **Prathamesh F**, Vijaysinh M. Platelet concentrates - preparation protocols and recent advances. *Int J Sci Res* 2010; **9**: 1-3 [DOI: 10.36106/ijsr/5018085]

36 **Gil A**, Bakhshalian N, Min S, Zadeh HH. Treatment of multiple recession defects with vestibular incision subperiosteal tunnel access (VISTA): A retrospective pilot study utilizing digital analysis. *J Esthet Restor Dent* 2018; **30**: 572-579 [PMID: 30367715 DOI: 10.1111/jerd.12434]

37 **Shah R**, Gowda TM, Thomas R, Kumar T, Mehta DS. Biological activation of bone grafts using injectable platelet-rich fibrin. *J Prosthet Dent* 2019; **121**: 391-393 [PMID: 30409723 DOI: 10.1016/j.prosdent.2018.03.027]

38 **Choukroun J**, Ghanaati S. Reduction of relative centrifugation force within injectable platelet-rich-fibrin (PRF) concentrates advances patients' own inflammatory cells, platelets and growth factors: the first introduction to the low speed centrifugation concept. *Eur J Trauma Emerg Surg* 2018; **44**: 87-95 [PMID: 28283682 DOI: 10.1007/s00068-017-0767-9]

39 **Ghanaati S**, Booms P, Orlowska A, Kubesch A, Lorenz J, Rutkowski J, Landes C, Sader R, Kirkpatrick C, Choukroun J. Advanced platelet-rich fibrin: a new concept for cell-based tissue engineering by means of inflammatory cells. *J Oral Implantol* 2014; **40**: 679-689 [PMID: 24945603 DOI: 10.1563/aaid-joi-D-14-00138]

40 **Mourão CF**, Valiense H, Melo ER, Mourão NB, Maia MD. Obtention of injectable platelets rich-fibrin (i-PRF) and its polymerization with bone graft: technical note. *Rev Col Bras Cir* 2015; **42**: 421-423 [PMID: 26814997 DOI: 10.1590/0100-69912015006013]

41 **Dohan Ehrenfest DM**, Del Corso M, Diss A, Mouhyi J, Charrier JB. Three-dimensional architecture and cell composition of a Choukroun's platelet-rich fibrin clot and membrane. *J Periodontol* 2010; **81**: 546-555 [PMID: 20373539 DOI: 10.1902/jop.2009.090531]

42 **Varela HA**, Souza JCM, Nascimento RM, Araújo RF Jr, Vasconcelos RC, Cavalcante RS, Guedes PM, Araújo AA. Injectable platelet rich fibrin: cell content, morphological, and protein characterization. *Clin Oral Investig* 2019; **23**: 1309-1318 [PMID: 30003342 DOI: 10.1007/s00784-018-2555-2]

43 **İzol BS**, Üner DD. A New Approach for Root Surface Biomodification Using Injectable Platelet-Rich Fibrin (I-PRF). *Med Sci Monit* 2019; **25**: 4744-4750 [PMID: 31241048 DOI: 10.12659/MSM.915142]

44 **Ucak Turer O**, Ozcan M, Alkaya B, Surmeli S, Seydaoglu G, Haytac MC. Clinical evaluation of injectable platelet-rich fibrin with connective tissue graft for the treatment of deep gingival recession defects: A controlled randomized clinical trial. *J Clin Periodontol* 2020; **47**: 72-80 [PMID: 31518440 DOI: 10.1111/jcpe.13193]

45 **Ozsagir ZB**, Saglam E, Sen Yilmaz B, Choukroun J, Tunali M. Injectable platelet-rich fibrin and microneedling for

gingival augmentation in thin periodontal phenotype: A randomized controlled clinical trial. *J Clin Periodontol* 2020; **47**: 489-499 [PMID: 31912532 DOI: 10.1111/jcpe.13247]

46 **Al-Maawi S**, Herrera-Vizcaíno C, Orlowska A, Willershausen I, Sader R, Miron RJ, Choukroun J, Ghanaati S. Biologization of Collagen-Based Biomaterials Using Liquid-Platelet-Rich Fibrin: New Insights into Clinically Applicable Tissue Engineering. *Materials (Basel)* 2019; **12**: 3993 [PMID: 31810182 DOI: 10.3390/ma12233993]

47 **Chai J**, Jin R, Yuan G, Kanter V, Miron RJ, Zhang Y. Effect of Liquid Platelet-rich Fibrin and Platelet-rich Plasma on the Regenerative Potential of Dental Pulp Cells Cultured under Inflammatory Conditions: A Comparative Analysis. *J Endod* 2019; **45**: 1000-1008 [PMID: 31248700 DOI: 10.1016/j.joen.2019.04.002]

48 **Bennardo F**, Liborio F, Barone S, Antonelli A, Buffone C, Fortunato L, Giudice A. Efficacy of platelet-rich fibrin compared with triamcinolone acetonide as injective therapy in the treatment of symptomatic oral lichen planus: a pilot study. *Clin Oral Investig* 2021; **25**: 3747-3755 [PMID: 33415379 DOI: 10.1007/s00784-020-03702-w]

49 **Kriti V**, Triveni G, Kumar AB, Mehta DS. Minimally Invasive Treatment of Mandibular Anterior Lingual Defects by Vestibular Incision Subperiosteal Tunnel Access (VISTA Technique) and Connective Tissue Graft: A Case Report. *Clin Adv Periodontics* 2017; **7**: 1-14 [DOI: 10.1902/cap.2017.170020]

50 **Reddy S**, Prasad MGS, Bhowmik N, Singh S, Pandit HR, Vimal SK. Vestibular incision subperiosteal tunnel access (VISTA) with platelet rich fibrin (PRF) and connective tissue graft (CTG) in the management of multiple gingival recession- A case series. *Int J Appl Dent Sci* 2016; **2**: 34-37

51 **Agarwal MC**, Rathore P, Gummaluri SS, Agarwal P, Kumari S. Vestibular Incision Subperiosteal Tunnel Access with Titanium-Prepared Platelet-Rich Fibrin - A Golden Approach for Treating Multiple Recession Defects in Esthetic Zone. *Contemp Clin Dent* 2019; **10**: 682-685 [PMID: 32792832 DOI: 10.4103/ccd.ccd_2_19]

52 **Pawar B**, Bhuse K, Shetty A, Shetty D. A Fantastic Approach for Multiple Recession Coverage: Vestibular Incision Subperiosteal Tunnel Access Technique (Vista)-A Case Report. *IOSR J Dent Med Sci* 2016; **15**: 52-56

53 **Geeti G**, Komal P, Mansi B, Manish K, Ashish K. Platelet Rich Fibrin (PRF) Reinforced Vestibular Incision Subperiosteal Tunnel Access (VISTA) Technique for Recession Coverage. *Clin Adv Periodontics* 2014; **5**: 248-253 [DOI: DOI:10.1902/cap.2014.140027]

54 **S RR**, Kumar TA, Gowda TM, Mehta DS, Kumar A. Management of Multiple Gingival Recessions with the VISTA Technique: An 18-Month Clinical Case Series. *Int J Periodontics Restorative Dent* 2018; **38**: 245-251 [PMID: 29447318 DOI: 10.11607/prd.2990]

55 **Tuttle D**, Kurtzman G, Bernotti AL. Gum Drop Technique: Minimally Invasive Soft-Tissue Platelet-Rich Plasma Grafting for Marginal Soft-Tissue Recession. *Compend Contin Educ Dent* 2018; **39**: e9-e12 [PMID: 29714492]

Published by **Baishideng Publishing Group Inc**
7041 Koll Center Parkway, Suite 160, Pleasanton, CA 94566, USA
Telephone: +1-925-3991568
E-mail: bpgoffice@wjgnet.com
Help Desk: https://www.f6publishing.com/helpdesk
https://www.wjgnet.com